

Data-Driven Bandit Learning for Proactive Cache Placement in Fog-Assisted IoT Systems

Xin Gao, *Student Member, IEEE*, Xi Huang, *Student Member, IEEE*, Yinxu Tang, Ziyu Shao*, *Senior Member, IEEE*, Yang Yang, *Fellow, IEEE*

Abstract—In Fog-assisted IoT systems, it is a common practice to cache popular content at the network edge to achieve high quality of service. Due to uncertainties in practice such as unknown file popularities, cache placement scheme design is still an open problem with unresolved challenges: 1) how to maintain time-averaged storage costs under budgets, 2) how to incorporate online learning to aid cache placement to minimize performance loss (*a.k.a.* regret), and 3) how to exploit offline history information to further reduce regret. In this paper, we formulate the cache placement problem with unknown file popularities as a constrained combinatorial multi-armed bandit (CMAB) problem. To solve the problem, we employ virtual queue techniques to manage time-averaged constraints, and adopt data-driven bandit learning methods to integrate offline history information into online learning to handle exploration-exploitation tradeoff. With an effective combination of online control and data-driven online learning, we devise a Cache Placement scheme with Data-driven Bandit Learning called **CPDBL**. Our theoretical analysis and simulations show that **CPDBL** achieves a sublinear time-averaged regret under long-term storage cost constraints.

Index Terms—Internet of Things, proactive caching, fog computing, data-driven bandit learning, learning-aided online control.

I. INTRODUCTION

During recent years, the proliferation of *Internet of Things* (IoT) devices such as smart phones and the emerging of IoT applications such as video streaming have led to the unprecedented growth of data traffic[1]. To meet the explosively growing traffic demands at the network edge and facilitate IoT applications with high *quality of service* (QoS), caching popular contents at fog nodes has emerged as a promising solution[2–5]. Figure 1 shows an example of wireless caching in a multi-tier Fog-assisted IoT system. As shown in the figure, by utilizing the storage resources on fog nodes that are close to IoT devices, popular contents (*e.g.*, files) can be cached to achieve timely content delivery. Due to resource limit, each edge fog server (EFS) can cache only a subset of files to serve its associated IoT users. If a user’s requested file is found on the corresponding EFS (*a.k.a.* a *hit*), then it can be downloaded directly; however, if not found on the EFS (*a.k.a.* a *miss*), then the file needs to be fetched from the central fog server (CFS) in the upper fog tier with extra bandwidth consumption and latency. Therefore, the key to maximize the effectiveness of caching in Fog-assisted IoT systems lies in the selection of

X. Gao, X. Huang, Y. Tang, Z. Shao, Y. Yang are with the School of Information Science and Technology, ShanghaiTech University, Shanghai 201210, China. (E-mail: {gaoxin, huangxi, tangyx, shaozy, yangyang}@shanghaitech.edu.cn) (*Corresponding author: Ziyu Shao)

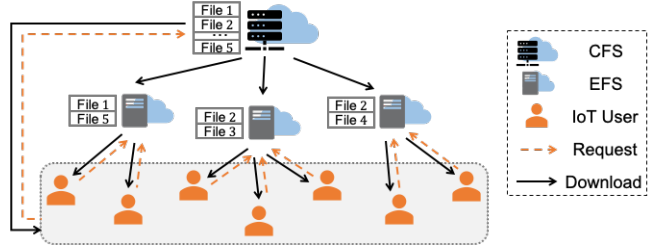


Fig. 1. An illustration of caching-enabled Fog-assisted IoT systems.

the proper set of cached files (*a.k.a.* *cache placement*) on each EFS.

However, the effective design of cache placement scheme remains as an open problem due to the uncertainty of file popularities in such systems. Specifically, as an important ingredient for cache placement optimization, file popularities are usually unknown *a priori* in practice[16]. Such information can only be inferred implicitly from feedback information such as cache hit signals for user requests. Besides, in practice, it is common for Fog-assisted IoT systems to retain offline historical observations about file popularity (in terms of file request logs) on each EFS. Such offline information can be exploited to reduce the uncertainty of file popularities in the procedure of cache placement. However, it remains non-trivial about how to integrate online feedback and offline history information to reduce uncertainties in decision making and minimize the resulting performance loss (*a.k.a.* regret). If such an integration can be well achieved, then each EFS can proactively update cache placement based on its learned popularity statistics to improve system performance.

Towards such a joint design, three challenges must be addressed. The first is concerning the tradeoff between conflicting performance metrics. On one hand, caching more popular files on each EFS conduces to higher *cache hit rewards* (*e.g.*, the size of files served by wireless caching). On the other hand, the number of cached files should be limited to avoid excessive *storage costs* (*e.g.*, memory footprint). Such a tradeoff between cache hit rewards and storage costs should be carefully considered for cache placement. The second is regarding the *exploration-exploitation* dilemma encountered in the online learning procedure; *i.e.*, for each EFS, should it cache the files with empirically high estimated popularities (exploitation) or those files with few collected feedbacks but potentially high popularities (exploration)? The third is about how to leverage offline history information to further improve

TABLE I. Comparison between our work and related works

	Optimization Metrics	Resource Constraints		Online Control	Online Learning	Offline History Information
		Per-time-slot Constraints	Long-term Constraints			
[6]	Revenue and cost of caching & delivery cost	•	•	•		
[7]	Service rates for file requests	•	•	•		
[8]	Queueing delay & energy consumption	•	•	•		
[9]	Task delay & energy consumption	•	•	•		
[10]	Cache hit reward	•			•	
[11]	Cache hit reward & file downloading cost	•			•	
[12]	Number of cache hits	•			•	
[13]	Weighted network utility	•			•	
[14]	Revenue of caching & content sharing cost	•			•	
[15]	Network transmission delay	•			•	
Our Work	Cache hit reward & storage cost	•	•	•	•	•

learning efficiency. With such a new degree of freedom in the design space of cache placement, the interplay among online control, online learning, and offline history information deserves a systematic investigation.

In this paper, we focus on the problem of proactive cache placement in caching-enabled Fog-assisted IoT systems with offline history information and unknown file popularities under long-term time-averaged constraints on storage costs of EFSs. We summarize our contributions and key results as follows.

◊ **Problem Formulation:** We formulate the problem as a stochastic optimization problem, which aims to maximize the total cache hit reward in terms of the amount of files directly fetched from EFSs to IoT users over a finite time horizon. Meanwhile, we also consider the time-averaged storage cost constraint on each EFS. By exploiting the problem structure, we extend the settings of the recently developed bandit model [17] and reformulate the problem as a constrained combinatorial multi-armed bandit (CMAB) problem.

◊ **Algorithm Design:** To solve the formulated problem, we propose *CPDBL* (Cache Placement with Data-driven Bandit Learning), a learning-aided cache placement scheme that conducts proactive cache placement under long-term time-averaged storage cost constraints. In general, CPDBL consists of two interacting procedures: the online learning procedure and the cache update procedure. Particularly, in the online learning procedure, we adopt HUCB1 (UCB1 with Historic Data) method [18] to leverage both offline history and online feedback to learn the unknown file popularities with a decent exploration-exploitation tradeoff. In the cache update procedure, we leverage Lyapunov optimization method [19] to update cached files on EFSs in an adaptive manner, aiming to maximize cache hit rewards while subject to long-term constraints on storage costs.

◊ **Theoretical Analysis:** To the best of our knowledge, our work conducts the first systematic study on the integration of online control, online learning, and offline history information. In particular, our theoretical analysis shows that our devised scheme achieves a near-optimal total cache hit reward under time-averaged storage cost constraints with a time-averaged regret of order $O(1/V + \sqrt{(\log T)/(T + H_{\min})})$ over a finite time horizon T . Note that V is a positive tunable parameter and H_{\min}

is the minimum number of offline historical observations among different EFSs.

- ◊ **Numerical Evaluation:** We conduct extensive simulations to investigate the performance of CPDBL and its variants. Our simulation results not only verify our theoretical analysis but also demonstrate the effectiveness of CPDBL in terms of regret minimization under long-term time-averaged constraints on storage costs.
- ◊ **New Degree of Freedom in the Design Space of Fog-Assisted IoT Systems:** We systematically investigate the fundamental benefits of offline history information in Fog-assisted IoT systems. We provide both theoretical analysis and numerical evaluations to verify such benefits.

The rest of this paper is organized as follows. Section II discusses the related works. Section III illustrates our system model and problem formulation. Section IV shows our algorithm design, followed by its performance analysis in Section V. Section VI discusses our simulation results and Section VII concludes this paper.

II. RELATED WORK

In the past decades, cache placement has been widely studied to improve the performance of wireless networks such as IoT networks and cellular networks[20]. Among existing works, those that are most relevant to our work are generally carried out from two perspectives: the *online control* perspective and the *online learning* perspective.

Online Control based Cache Placement: Most works that take the online control perspective formulated cache placement problems as stochastic network optimization problems with respect to different metrics. For example, in [6] Pang *et al.* jointly studied the cache placement and data sponsoring problems in mobile video content delivery networks. Their solution aimed to maximize the overall content delivery payoff with budget constraints on caching and delivery costs. Kwak *et al.*[7] devised a dynamic cache placement scheme to optimize service rates for user requests in a hierarchical wireless caching network. Wang *et al.*[8] developed a joint traffic forwarding and cache placement scheme to optimize the queueing delay and energy consumption of cache-enabled networks. In [9], Xu *et al.* proposed an online algorithm to jointly optimize wireless caching and task offloading with the goal of ultra-low task computation delay under a long-term energy constraint. In general, such works adopted Lyapunov

optimization method[19] to solve their formulated problems through a series of per-time-slot adaptive control. Although the effectiveness of their solutions has been well justified, they generally assumed that file popularities or file requests are readily given upon cache placement. Such assumptions are usually not the case in practice[16].

Online Learning based Cache Placement: Faced with constantly arriving file requests and unknown file popularities, a number of works adopted various learning techniques such as deep learning[21], transfer learning[16][22], and reinforcement learning[10–15, 23, 24] to improve the performance of wireless caching networks. Nonetheless, such solutions mainly resort to offline pre-training procedures and can not provide theoretical performance guarantee in general.

Bandit learning is another method that is widely adopted to promote the performance of such systems. So far, it has been applied to solve scheduling problems such as task offloading[25], task allocation[26], and path selection[27]. The most relevant to our work are those which consider optimizing proactive cache placement in terms of different performance metrics. For example, Blasco *et al.*[10][11] studied the cache placement problem for a single caching unit with multiple users. By considering the problem as a CMAB problem, in [10] they aimed to maximize the amount of served traffic through wireless caching, while in [11] they further took file downloading costs into the account of optimization. In [12], Müller *et al.* proposed a cache placement scheme based on contextual bandits, which learns the context-dependent content popularity to maximize the number of cache hits. Song *et al.*[14] proposed a joint cache placement and content sharing scheme among cooperative caching units to maximize the content caching revenue and minimize the content sharing expense. Zhang *et al.*[13] studied the network utility maximization problem in the context of cache placement with a non-fixed content library over time. In [15], Xu *et al.* modeled the procedure of cache placement with multiple caching units from the perspective of multi-agent multi-armed bandit (MAMAB) and devised an online scheme to minimize the accumulated transmission delay over time. Note that the above works generally do not consider the storage costs on EFSs in terms of memory footprint. However, in practice, without such a consideration, caching files with excessively high storage costs may offset the gains of wireless caching. Moreover, none of such works exploits offline history information in their learning processes.

Novelty of Our Work: Different from existing works, to our best knowledge, our work presents the first systematic study on the synergy of online control, online learning, and offline history information. In particular, we conduct theoretical analysis to characterize the joint impacts of online control, online learning, and offline information on the performance of cache placement. Our results also provide novel insights to the designers of Fog-assisted IoT systems. The comparison between our work and existing works is given in Table I.

III. SYSTEM MODEL AND PROBLEM FORMULATION

In this Section, we describe our system model in detail. Then we formulate the cache placement problem as a

TABLE II. Key notations

Notation	Description
T	Total number of time slots
\mathcal{N}	Set of EFSs with $ \mathcal{N} \triangleq N$
\mathcal{K}	Set of IoT users with $ \mathcal{K} \triangleq K$
\mathcal{K}_n	Set of IoT users served by EFS n
\mathcal{F}	Set of files with $ \mathcal{F} \triangleq F$
L_f	Size of file f
M_n	Storage capacity of EFS n
$\theta_{k,f}(t)$	Indicator of whether file f is requested by IoT user k in time slot t
$D_{n,f}(t)$	Total number of IoT users in set \mathcal{K}_n who request for file f in time slot t
$d_{n,f}$	Popularity of file f on EFS n , $d_{n,f} \triangleq \mathbb{E}[D_{n,f}(t)]$
$H_{n,f}$	Number of offline historical observations available for the popularity of file f on EFS n
$D_{n,f}^h(s)$	Total number of IoT users in set \mathcal{K}_n who request for file f recorded by the s th offline historical observation
$\hat{d}_{n,f}(t)$	Estimated popularity of file f on EFS n in time slot t
$X_{n,f}(t)$	Cache placement decision for caching file f on EFS n in time slot t
$C_n(t)$	Storage cost of EFS n in time slot t
$R_{n,f}(t)$	Cache hit reward of EFS n with respect to file f in time slot t
$R_n(t)$	Total cache hit reward of EFS n in time slot t
b_n	Storage cost budget for EFS n

stochastic optimization problem with long-term constraints. Key notations in this paper are summarized in Table II.

A. Basic Model

We consider a caching-enabled Fog-assisted IoT system that operates over a finite time horizon of T time slots. In the system, there is a central fog server (CFS) which manages N edge fog servers (EFSs) to serve K IoT users. We denote the sets of EFSs and users by $\mathcal{N} \triangleq \{1, 2, \dots, N\}$ and $\mathcal{K} \triangleq \{1, 2, \dots, K\}$, respectively. For each EFS n , we define \mathcal{K}_n ($\mathcal{K}_n \subseteq \mathcal{K}$, $|\mathcal{K}_n| = K_n$) as the set of IoT users within its service range. Note that each IoT user is served by only one EFS and thus the sets $\{\mathcal{K}_n\}_n$ are disjoint.

Particularly, we focus on the scenario in which IoT users request to download files from EFSs. We assume that the CFS has stored all of F files (denoted by set $\mathcal{F} \triangleq \{1, 2, \dots, F\}$) that could be requested within the time horizon. Each file f has a fixed size of L_f storage units. Due to caching capacity limit, each EFS n only has M_n units of storage to cache a portion of the files and $M_n < \sum_{f \in \mathcal{F}} L_f$. Accordingly, if a user cannot find its requested file on its associated EFS, it will request to download the file directly from the CFS. We show an example to illustrate our system model in Figure 1.

B. File Popularity

On each EFS n , we define the popularity of each file f as the expected number of users to request file f (denoted by $d_{n,f}$) per time slot. We assume that each file's popularity

remains constant within the time horizon. In practice, such file popularities are usually unknown *a priori* and can only be inferred based on online feedback information collected after user requests have been served.

Next, we introduce some variables to characterize user dynamics with respect to file popularity. We define binary variable $\theta_{k,f}(t) \in \{0, 1\}$ such that $\theta_{k,f}(t) = 1$ if IoT user k requests for file f in time slot t and zero otherwise. Then we denote the file requests of IoT user k during time slot t by vector $\boldsymbol{\theta}_k(t) \triangleq (\theta_{k,1}(t), \theta_{k,2}(t), \dots, \theta_{k,F}(t))$. Meanwhile, we use $D_{n,f}(t) \triangleq \sum_{k \in \mathcal{K}_n} \theta_{k,f}(t)$ to denote the total number of IoT users in set \mathcal{K}_n who request for file f on EFS n in time slot t . Note that $D_{n,f}(t)$ is a discrete random variable over support set $\{0, 1, \dots, K_n\}$ and assumed to be *i.i.d.* across time slots with a mean of $d_{n,f}$.

Besides, we assume that offline historical observations with respect to the requests for each file f are available on each EFS n . Specifically, the offline historical observations for file f on EFS n are denoted by $\{D_{n,f}^h(0), D_{n,f}^h(1), \dots, D_{n,f}^h(H_{n,f} - 1)\}$, where $H_{n,f} \geq 1$ denotes the number of offline historical observations available for file f on EFS n . Note that we use superscript h to indicate that $D_{n,f}^h(s)$ belongs to offline history information. When $H_{n,f} = 0$, there is no offline history information. The offline historical observations are assumed to follow the same distribution as the current file popularities.

C. System Workflow

During each time slot t , the system operates across two phases: the caching phase and the service phase.

- ◊ *Caching phase*: At the beginning of time slot t , each EFS n updates its cached files and consumes a storage cost for each cached file. Then each EFS n broadcasts its cache placement to all IoT users in set \mathcal{K}_n .
- ◊ *Service phase*: Each IoT user generates file requests and sends them to its associated EFS. For each request, if the requested file is not found on the EFS, then the user will turn to fetch the file from the CFS. Otherwise, the user directly downloads the file from the EFS. Meanwhile, the EFS will receive a corresponding cache hit reward.

In the next few subsections, we present the definitions of cache placement decisions, storage costs, and cache hit rewards in detail, respectively.

D. Cache Placement Decision

For each EFS n , we denote its cache placement decision made during each time slot t by a binary vector $\boldsymbol{X}_n(t) \triangleq (X_{n,1}(t), X_{n,2}(t), \dots, X_{n,F}(t))$. Each entry $X_{n,f}(t) = 1$ if EFS n decides to cache file f during time slot t and zero otherwise. Note that the total size of cached files on EFS n does not exceed its storage capacity, *i.e.*,

$$\sum_{f \in \mathcal{F}} L_f X_{n,f}(t) \leq M_n, \quad \forall n \in \mathcal{N}, t. \quad (1)$$

E. Storage Cost

For each EFS n , caching file f during a time slot t will incur a storage cost of αL_f , where $\alpha > 0$ is the unit storage

cost. The storage cost can be viewed as the memory footprint for maintaining the file which is proportional to the size of file f . Accordingly, given decision $\boldsymbol{X}_n(t)$, we define the total storage cost on EFS n during time slot t as

$$C_n(t) \triangleq \sum_{f \in \mathcal{F}} \alpha L_f X_{n,f}(t). \quad (2)$$

F. Cache Hit Reward

Recall that during each time slot t , for *each* requested file f , if $X_{n,f}(t) = 1$, then EFS n will receive a reward L_f for the corresponding cache hit [10] (in terms of amounts of traffic to fetch file f from EFS n). Then given cache placement $X_{n,f}(t)$ and user demand $D_{n,f}(t)$ during time slot t , we define the cache hit reward of EFS n with respect to file f as

$$R_{n,f}(t) \triangleq L_f D_{n,f}(t) X_{n,f}(t). \quad (3)$$

Note that the cache hit reward $R_{n,f}(t) = 0$ if file f is not cached on EFS n during time slot t (*i.e.*, when $X_{n,f}(t) = 0$). Accordingly, we define the total cache hit reward of EFS n during time slot t as

$$R_n(t) \triangleq \hat{R}_n(\boldsymbol{X}_n(t)) \triangleq \sum_{f \in \mathcal{F}} L_f D_{n,f}(t) X_{n,f}(t). \quad (4)$$

G. Problem Formulation

To achieve effective cache placement with high QoS, two goals are considered in our work. One is to maximize the total size of transmitted files from all EFSs so as to ensure requests from IoT users should receive timely service. In our model, this is equivalent to maximizing the time-averaged cache hit reward of all EFSs over a time horizon of T time slots. The other is to guarantee a budgeted usage of storage costs over time. To this end, for each EFS n , we first define b_n as the long-term storage cost budget for caching files. Then we impose the following constraint to keep the time-averaged storage costs under the budget in the long run:

$$\limsup_{t \rightarrow \infty} \frac{1}{t} \sum_{\tau=0}^{t-1} \mathbb{E}[C_n(\tau)] \leq b_n, \quad \forall n \in \mathcal{N}. \quad (5)$$

Based on the above system model and constraints, our problem formulation is given by

$$\underset{\{\boldsymbol{X}(t)\}_t}{\text{maximize}} \quad \frac{1}{T} \sum_{t=0}^{T-1} \sum_{n \in \mathcal{N}} \mathbb{E}[R_n(t)] \quad (6a)$$

$$\text{subject to} \quad X_{n,f}(t) \in \{0, 1\}, \quad \forall n \in \mathcal{N}, f \in \mathcal{F}, t, \quad (6b)$$

$$(1), (5).$$

In the above formulation, the objective (6a) is to maximize the time-averaged expectation of total cache hit reward of all EFSs. Constraint (6b) states that each cache placement decision $X_{n,f}(t)$ should be a binary variable. Constraint (1) guarantees that the total size of cached files on each EFS should not exceed the storage capacity. Constraint (5) ensures the budget constraint on the storage costs of each EFS.

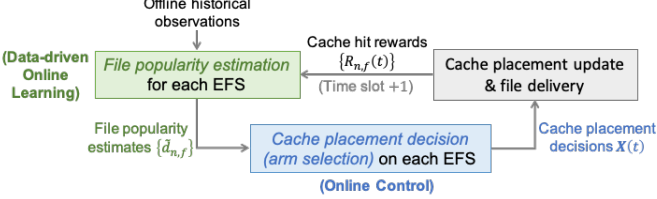


Fig. 2. An illustration of our algorithm design.

IV. ALGORITHM DESIGN

For problem (6), given the full knowledge of user demands $\{D_{n,f}(t)\}_{n,f}$, it can be solved asymptotically optimally by Lyapunov optimization methods [19]. However, file popularities are usually unknown *a priori* in practice. Faced with such uncertainties, online learning needs to be incorporated to guide the decision-making process by fitting the statistics of file popularities from both online feedback and offline history information. To this end, we need to deal with the well-known *exploration-exploitation* dilemma, *i.e.*, how to balance the decisions made to acquire new knowledge about file popularity to improve learning accuracy (*exploration*) and the decisions made to leverage current knowledge to select the empirically most popular files (*exploitation*). For such a decision-making problem under uncertainty, we consider it through the lens of combinatorial multi-armed bandit (CMAB) with extended settings. With an effective integration of online bandit learning, online control, and offline history information, we devise a data-driven learning-aided cache placement scheme CPDBL (Cache Placement with Data-driven Bandit Learning) to solve problem (6). Figure 2 depicts the design of CPDBL. During each time slot, under CPDBL, each EFS first estimates the popularity of different files based on both offline history information and collected online feedback. With such estimates, the EFS determines and updates its cache placement in the current time slot. After the update, each EFS delivers requested cached files to IoT users. For each cache hit, a reward will be credited to the EFS.

In the following subsections, we extend the settings of the existing CMAB model and demonstrate the reformulation of problem (6) under such settings. Then we articulate our algorithm design with respect to online learning and online control procedures, respectively. Finally, we discuss the computational complexity of our devised algorithm.

A. Problem Reformulation

The basic settings of CMAB [28] consider a sequential interaction between a player and its environment with multiple actions (*a.k.a.* arms) over a finite number of rounds. During each round, the player selects a subset of available arms to play. Then the environment reveals to each selected arm with a reward that is sampled from an unknown distribution. The overall goal of the player is to find an effective arm-selection scheme to maximize its expected cumulative reward.

Based on the CMAB model, Li *et al.*[17] extended the settings of classical CMAB by allowing the temporary unavailability of arms while considering the fairness of arm

selection. Inspired by their work, we reformulate problem (6) as a constrained CMAB problem in the following way. We view each EFS as a distinct player and each file as an arm. During each time slot t , each player $n \in \mathcal{N}$ selects a subset of arms to play. If player n chooses to play arm $f \in \mathcal{F}$ in time slot t , then file f will be cached on EFS n and a reward $R_{n,f}(t) = L_f D_{n,f}(t)$ will be received by the player. Recall that the file demand $D_{n,f}(t)$ during each time slot t is a random variable with an unknown mean $d_{n,f}$ and *i.i.d.* across time slots. Accordingly, reward $R_{n,f}(t)$ is also an *i.i.d.* random variable with an unknown mean $r_{n,f} = \mathbb{E}[R_{n,f}(t)] = L_f d_{n,f}$. Meanwhile, the cache placement decision $\mathbf{X}_n(t) = (X_{n,1}(t), X_{n,2}(t), \dots, X_{n,F}(t))$ of EFS n corresponds to the arm selection of player n in time slot t . Specifically, $X_{n,f}(t) = 1$ if arm f is chosen and zero otherwise. Our goal is to devise an arm selection scheme for the players to maximize their expected cumulative reward while subject to constraints (1) and (5).

Remark: Our model extends the settings of the bandit model proposed by [17] in the following four aspects. First, we consider multiple players instead of one player. Second, the storage cost constraints in our problem are more complex than the arm fairness constraints in [17]. Specifically, under our settings, the selection of each arm for a player is coupled together under storage cost constraints, whereas in [17] there is no such coupling among arm selections. Third, we consider the storage capacity constraint for each player during each time slot, which is ignored in [17]. Last but not least, we consider a more general reward function with respect to file uncertainties. With above extensions, our reformulated problem is more challenging than the problem formulated in [17].

To characterize the performance loss (*a.k.a.* regret) due to decision making under such uncertainties, we define the regret with respect to a given scheme (denoted by decision sequence $\{\mathbf{X}(t)\}_t$) as

$$Reg(T) \triangleq R^* - \frac{1}{T} \sum_{t=0}^{T-1} \sum_{n \in \mathcal{N}} \mathbb{E} [\hat{R}_n(\mathbf{X}_n(t))], \quad (7)$$

where constant R^* is defined as the optimal time-averaged total expected reward for all players. In fact, maximizing the time-averaged expected reward is equivalent to minimizing the regret. Therefore, we can rewrite problem (6) as follows:

$$\underset{\{\mathbf{X}(t)\}_t}{\text{minimize}} \quad Reg(T) \quad (8a)$$

$$\text{subject to} \quad (1)(5)(6b). \quad (8b)$$

To solve problem (8), we integrate data-driven bandit learning methods and virtual queue techniques to handle the exploration-exploitation tradeoff and the long-term storage cost constraints, respectively. In the following subsections, we articulate our algorithm design in detail.

B. Online Bandit Learning with Offline History Information

By (4), the regret defined in (7) can be rewritten as

$$Reg(T) = R^* - \frac{1}{T} \sum_{t=0}^{T-1} \sum_{n \in \mathcal{N}} \sum_{f \in \mathcal{F}} L_f \mathbb{E} [D_{n,f}(t) X_{n,f}(t)]$$

$$= R^* - \frac{1}{T} \sum_{t=0}^{T-1} \sum_{n \in \mathcal{N}} \sum_{f \in \mathcal{F}} L_f d_{n,f} \mathbb{E}[X_{n,f}(t)], \quad (9)$$

where the last equality holds due to the independence between user demand $D_{n,f}(t)$ and cache placement $X_{n,f}(t)$, and the fact that $\mathbb{E}[D_{n,f}(t)] = d_{n,f}$. By (9) and our previous analysis, we know that to solve problem (8), each EFS n should learn the unknown file popularity $d_{n,f}$ with respect to each file f .

During each time slot t , after updating cached files according to decision $\mathbf{X}_n(t)$, each EFS n observes the current demand $D_{n,f}(t)$ for each cached file f . Then EFS n transmits requested files to IoT users and acquires cache hit rewards. Based on pre-given offline history information and cache hit feedback from IoT users, we have the following estimate for each file popularity $d_{n,f}$:

$$\tilde{d}_{n,f}(t) = \min \left\{ \bar{d}_{n,f}(t) + K_n \sqrt{\frac{3 \log t}{2(h_{n,f}(t) + H_{n,f})}}, K_n \right\}. \quad (10)$$

In (10), $\bar{d}_{n,f}(t)$ is the empirical mean of the number of requests for file f that involves both offline historical observations and collected online feedback; $h_{n,f}(t)$ counts the number of time slots (within the first t time slots) during which file f is chosen to be cached on EFS n ; and K_n denotes the number of users served by EFS n . Specifically, the number of observations $h_{n,f}(t)$ and the empirical mean of file popularity $\bar{d}_{n,f}(t)$ by time slot t are defined as follows, respectively:

$$h_{n,f}(t) \triangleq \sum_{\tau=0}^{t-1} X_{n,f}(\tau), \quad (11)$$

$$\bar{d}_{n,f}(t) \triangleq \frac{\sum_{\tau=0}^{t-1} D_{n,f}(\tau) X_{n,f}(\tau) + \sum_{s=0}^{H_{n,f}-1} D_{n,f}^h(s)}{h_{n,f}(t) + H_{n,f}}. \quad (12)$$

Remark: In (10), the term $K_n \sqrt{\frac{3 \log t}{2(h_{n,f}(t) + H_{n,f})}}$ is the *confidence radius*[29] that represents the degree of uncertainty for the empirical estimate $\tilde{d}_{n,f}(t)$. The larger the confidence radius, the greater the value of the estimate (10) and thus the greater the chance for file f to be cached on EFS n . In the confidence radius, the term $h_{n,f}(t) + H_{n,f}$ is the total number of observations (including both online observations and offline historical observations) for the popularity of file f on EFS n . Given a small number of observations (*i.e.*, $h_{n,f}(t) + H_{n,f} \ll t$), the confidence radius for the empirical estimate $\tilde{d}_{n,f}(t)$ will be large, which implies the file is rarely cached and hence a great uncertainty about the estimate. In this case, the confidence radius plays a dominant role in the estimate $\tilde{d}_{n,f}(t)$. Accordingly, file f will be more likely to be cached on EFS n . In contrast, when a file has been cached for an adequate number of times, then its popularity estimate (10) will be close to its empirical mean and the role of confidence radius will be marginalized. Besides, the HUCB1 estimate (10) also characterizes the effects of offline history information and online feedback information. Particularly, in the early stage (when t is small), suppose the number of online observations is much smaller than the number of offline historical observations, *i.e.*, $h_{n,f}(t) \ll H_{n,f}$. In this case, the HUCB1 estimate

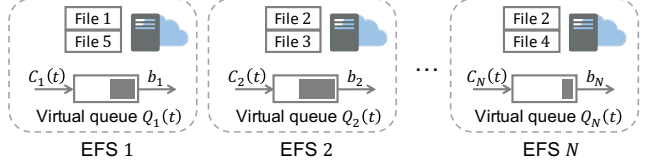


Fig. 3. An illustration of virtual queues for storage cost on each EFS. Each EFS $n \in \mathcal{N}$ maintains a virtual queue $Q_n(t)$ with an input of $C_n(t)$ and an output of b_n during each time slot t . If the queueing process $\{Q_n(t)\}_t$ is strongly stable, then the long-term time-averaged storage cost constraint (5) on EFS n can be satisfied.

mainly depends on offline history information. However, as more and more online feedbacks are collected, the impact of online information becomes more dominant.

C. Storage Cost Budgets with Virtual Queue Technique

By leveraging Lyapunov optimization techniques[19], we transform the long-term time-averaged storage cost constraints into queue stability constraints. Specifically, we introduce a virtual queue $Q_n(t)$ for each EFS $n \in \mathcal{N}$ with $Q_n(0) = 0$ to handle the time-averaged constraints (5) on storage costs. As illustrated in Figure 3, each virtual queue $Q_n(t)$ is updated during each time slot t as follows:

$$Q_n(t+1) = [Q_n(t) - b_n]^+ + C_n(t), \quad (13)$$

in which we define $[\cdot]^+ \triangleq \max\{\cdot, 0\}$. Note that constraints (5) are satisfied only when the queueing process $\{Q_n(t)\}_t$ for each EFS n is strongly stable [19]. Intuitively, the mean queue inputs (*i.e.*, storage costs) should not be greater than the mean queue outputs (*i.e.*, cost budgets). Otherwise, virtual queues will be overloaded, thereby violating constraint (5). To maintain the stability of virtual queues and minimize the regret, we transform problem (8) into a series of per-time-slot subproblems. Specifically, during each time slot t , we aim to solve the following problem for each EFS $n \in \mathcal{N}$:

$$\underset{\mathbf{X}_n(t)}{\text{maximize}} \sum_{f \in \mathcal{F}} \tilde{w}_{n,f}(t) X_{n,f}(t) \quad (14a)$$

$$\text{subject to} \quad \sum_{f \in \mathcal{F}} L_f X_{n,f}(t) \leq M_n, \quad (14b)$$

$$X_{n,f}(t) \in \{0, 1\}, \forall f \in \mathcal{F}, \quad (14c)$$

where $\tilde{w}_{n,f}(t)$ is defined as

$$\tilde{w}_{n,f}(t) \triangleq L_f (V \tilde{d}_{n,f}(t) - \alpha Q_n(t)). \quad (15)$$

In (15), parameter V is a tunable positive constant; weight $\tilde{w}_{n,f}(t)$ can be viewed as the gain of caching file f on EFS n during time slot t ; and the objective of problem (14) is to maximize the total gain of caching files on EFS n under the storage capacity constraint (14b).

During each time slot t , we solve problem (14) for each EFS n to determine its cache placement $\mathbf{X}_n(t)$. We split set \mathcal{F} into two disjoint sets $\mathcal{F}_{n,1}(t) = \{f \in \mathcal{F} : \tilde{w}_{n,f}(t) \geq 0\}$ and $\mathcal{F}_{n,2}(t) = \{f \in \mathcal{F} : \tilde{w}_{n,f}(t) < 0\}$ for each EFS n . Specifically, for each file $f \in \mathcal{F}$,

- 1) if $\tilde{d}_{n,f}(t) \geq \alpha Q_n(t)/V$, then $\tilde{w}_{n,f}(t) \geq 0$ and $f \in \mathcal{F}_{n,1}(t)$;

2) if $\tilde{d}_{n,f}(t) < \alpha Q_n(t)/V$, then $\tilde{w}_{n,f}(t) < 0$ and $f \in \mathcal{F}_{n,2}(t)$.

For each file $f \in \mathcal{F}_{n,2}(t)$, the corresponding optimal placement decision is $X_{n,f}(t) = 0$ since caching file f on EFS n will incur a negative gain, *i.e.*, $\tilde{w}_{n,f}(t) < 0$. By setting $X_{n,f}(t) = 0$ for each file $f \in \mathcal{F}_{n,2}(t)$, we can regard problem (14) as a classical Knapsack problem[30]

$$\begin{aligned} & \text{maximize}_{\{X_{n,f}(t)\}_{f \in \mathcal{F}_{n,1}(t)}} \sum_{f \in \mathcal{F}_{n,1}(t)} \tilde{w}_{n,f}(t) X_{n,f}(t) \\ & \text{subject to} \quad \sum_{f \in \mathcal{F}_{n,1}(t)} L_f X_{n,f}(t) \leq M_n, \\ & \quad X_{n,f}(t) \in \{0, 1\}, \forall f \in \mathcal{F}_{n,1}(t). \end{aligned} \quad (16)$$

Intuitively, from the lens of Knapsack problem, we have a number of items (files) in set $\mathcal{F}_{n,1}(t)$ and a knapsack (EFS n 's cache) with a capacity of M_n . The weight of each item $f \in \mathcal{F}_{n,1}(t)$ is L_f , while the value of putting item f in the knapsack is $\tilde{w}_{n,f}(t)$. Given the weights and values of all items, our goal is to select and put a subset of items from $\mathcal{F}_{n,1}(t)$ into the knapsack with the maximum total value. Such a problem can be solved optimally by applying dynamic programming (DP) algorithm [31].

D. Integrated Algorithm Design

Based on the design presented in the previous two subsections, we propose a novel learning-aided proactive cache placement scheme called CPDBL (Cache Placement with Data-driven Bandit Learning) and show its pseudocode in Algorithm 1. In particular, we denote the file indices in set $\mathcal{F}_{n,1}(t)$ by $\phi_{n,1}(t), \phi_{n,2}(t), \dots, \phi_{n,|\mathcal{F}_{n,1}(t)|}(t)$, respectively. We use $v(i, m)$ to denote the optimal value of problem (16) when only the first i files (*i.e.*, files indexed by $\phi_{n,1}(t), \dots, \phi_{n,i}(t)$) in $\mathcal{F}_{n,1}(t)$ can be selected. Regarding CPDBL, we have the following remarks.

Remark 1: In (15), the value of parameter V in weight $\tilde{w}_{n,f}(t)$ measures the relative importance of achieving high cache hit rewards to ensuring storage cost constraints. Note that the value of $\tilde{w}_{n,f}(t)$ is positively proportional to the value of parameter V . Therefore, for each file $f \in \mathcal{F}$, the gain $\tilde{w}_{n,f}(t)$ of caching file f on EFS n during time slot t will increase as the value of V increases. Under CPDBL, EFS n will cache more files to achieve not only a higher gain but also a larger storage cost. Moreover, files with high estimated mean cache hit rewards would be the first to be cached.

Remark 2: To ensure the storage cost constraints (5), CPDBL would restrict each EFS to cache limited files as its virtual queue backlog size becomes large. Intuitive, for each EFS n , if its time-averaged storage cost tends to exceed the cost budget b_n , its corresponding virtual queue backlog size $Q_n(t)$ will be large. By the definition of $\tilde{w}_{n,f}(t)$ in (15), the value of $\tilde{w}_{n,f}(t)$ is negatively proportional to the virtual queue backlog size $Q_n(t)$. Therefore, when the value of $Q_n(t)$ increases, the gain $\tilde{w}_{n,f}(t)$ of caching file f on EFS n tends to be negative. Under CPDBL, files with negative weights will not be cached, which conduces to a low time-averaged storage cost.

Algorithm 1 Cache Placement with Data-driven Bandit Learning (CPDBL)

```

1: Initialize  $h_{n,f}(0) = 0$ ,  $\tilde{d}_{n,f}(0) = \frac{1}{H_{n,f}} \sum_{s=1}^{H_{n,f}} D_{n,f}^h(s)$  and
    $\tilde{d}_{n,f}(0) = K_n$  for each EFS  $n \in \mathcal{N}$  and each file  $f \in \mathcal{F}$ . In
   each time slot  $t \in \{0, 1, \dots\}$ :
   %Data-driven Online Learning
2: for each EFS  $n \in \mathcal{N}$  and each file  $f \in \mathcal{F}$  do
3:   if  $h_{n,f}(t) > 0$  then
4:      $\tilde{d}_{n,f}(t) \leftarrow \min \left\{ \tilde{d}_{n,f}(t) + K_n \sqrt{\frac{3 \log t}{2(h_{n,f}(t) + H_{n,f})}}, K_n \right\}$ .
5:   end if
6: end for
   %Cache Placement
7: for each EFS  $n \in \mathcal{N}$  do
8:   SETCACHEPLACEMENT( $t, n, \{\tilde{d}_{n,f}(t)\}_{n,f}$ ).
9: end for
   %Update of Selection Counts and Empirical Means
10: Update cached content according to  $\mathbf{X}(t)$  and virtual queues
     $\mathbf{Q}(t)$  according to (13).
11: for each EFS  $n \in \mathcal{N}$  and each file  $f \in \mathcal{F}$  do
12:    $h_{n,f}(t) \leftarrow h_{n,f}(t-1) + X_{n,f}(t)$ .
13:    $\tilde{d}_{n,f}(t) \leftarrow \frac{h_{n,f}(t-1) + H_{n,f}}{h_{n,f}(t) + H_{n,f}} \tilde{d}_{n,f}(t-1) + \frac{D_{n,f}^h(t) X_{n,f}(t)}{h_{n,f}(t) + H_{n,f}}$ .
14: end for

```

E. Computational Complexity of CPDBL

The computational complexity of CPDBL mainly lies in the decision making for cache placement on each EFS $n \in \mathcal{N}$ (line 8 in Algorithm 1). In this process, DP is adopted to solve problem (14) with a computational complexity of $O(FM_n)$ [31]. Note that F denotes the total number of files on the CFS and M_n denotes the storage capacity of EFS n . In practice, the cache placement procedure can proceed in a distributed fashion over different EFNs; accordingly, the total computational complexity of CPDBL is $O(F \max_{n \in \mathcal{N}} M_n)$.

```

1: function SETCACHEPLACEMENT( $t, n, \{\tilde{d}_{n,f}(t)\}_{n,f}$ )
2:   Inputs: At the beginning of time slot  $t$ , for EFS  $n$ , given file
    demand estimate  $\{\tilde{d}_{n,f}(t)\}_{n,f}$ .
3:   Set  $\mathcal{F}_{n,1}(t) \leftarrow \emptyset$ .
4:   for each file  $f \in \mathcal{F}$  do
5:     Set  $\tilde{w}_{n,f}(t) \leftarrow L_f (V \tilde{d}_{n,f}(t) - Q_n(t))$ .
6:     if  $\tilde{w}_{n,f}(t) < 0$  then
7:       Set  $X_{n,f}(t) \leftarrow 0$ .
8:     else
9:       Set  $\mathcal{F}_{n,1}(t) \leftarrow \mathcal{F}_{n,1}(t) \cup \{f\}$ .
10:    end if
11:   end for
12:   Initialize  $v_n(i, m) = 0$  for  $i \in \{0, 1, 2, \dots, |\mathcal{F}_{n,1}(t)|\}$  and
     $m \in \{0, 1, \dots, M_n\}$ .
13:   for each  $i \in \{1, 2, \dots, |\mathcal{F}_{n,1}(t)|\}$  do
14:     for each  $m \in \{1, \dots, M_n\}$  do
15:       if  $L_{\phi_{n,i}(t)} > m$  then
16:         Set  $v_n(i, m) \leftarrow v_n(i-1, m)$ .
17:       else
18:         Set  $v_n(i, m) \leftarrow \max \{v_n(i-1, m), v_n(i-1, m - L_{\phi_{n,i}(t)}) + \tilde{w}_{n,\phi_{n,i}(t)}(t)\}$ .
19:       end if
20:     end for
21:   end for
22:   FINDOPTPLACEMENT( $n, |\mathcal{F}_{n,1}(t)|, M_n$ ).
23: end function

```

```

1: function FINDOPTPLACEMENT( $n, i, m$ )
2:   Inputs: For EFS  $n$ , given the number of files  $i$  and the
   remaining storage size  $m$ .
3:   if  $i \geq 1$  then
4:     if  $v_n(i, m) = v_n(i-1, m - L_{\phi_n, i}(t)) + \tilde{w}_{n, \phi_n, i}(t)$  and
        $m - L_{\phi_n, i}(t) \geq 0$  then
5:       Set  $X_{n, \phi_n, i}(t) \leftarrow 1$ .
6:       FINDOPTPLACEMENT( $n, i-1, m - L_{\phi_n, i}(t)$ ).
7:     else if  $v_n(i, m) = v_n(i-1, m)$  then
8:       Set  $X_{n, \phi_n, i}(t) \leftarrow 0$ .
9:       FINDOPTPLACEMENT( $n, i-1, m$ ).
10:    end if
11:   end if
12: end function

```

V. PERFORMANCE ANALYSIS

For each EFS n , given the number K_n of its served users and its storage capacity M_n , as well as the size L_f of each file $f \in \mathcal{F}$, we establish the following two theorems to characterize the performance of CPDBL.

A. Storage Cost Constraints

A budget vector $\mathbf{b} = (b_1, b_2, \dots, b_N)$ of storage costs is said to be *feasible* if there exists a feasible cache placement scheme under which all long-term time-averaged storage cost constraints can be satisfied. We define the set of all feasible budget vectors as the *maximal feasibility region* of the system. The following theorem shows that all virtual queues are strongly stable under CPDBL when \mathbf{b} is an interior point of the maximal feasibility region.

Theorem 1: Suppose that the budget vector \mathbf{b} lies in the interior of the maximal feasibility region of the system, then the long-term time-averaged storage cost constraints (5) are satisfied under CPDBL. Moreover, the virtual queues defined in (13) are strongly stable and there exists some constant $\epsilon > 0$ such that

$$\limsup_{t \rightarrow \infty} \frac{1}{t} \sum_{\tau=0}^{t-1} \sum_{n \in \mathcal{N}} \mathbb{E}[Q_n(\tau)] \leq \frac{B + V \sum_{n \in \mathcal{N}} 2K_n M_n}{\epsilon}, \quad (17)$$

where $B \triangleq \sum_{n \in \mathcal{N}} (b_n^2 + \alpha^2 M_n^2)/2$.

Remark 1: The proof of Theorem 1 is given in Appendix B. Theorem 1 shows that CPDBL ensures the stability of virtual queue backlogs $\{Q_n(t)\}_n$. Moreover, the time-averaged total backlog size of such virtual queues is linearly proportional to the value of parameter V . In other words, given that vector \mathbf{b} is interior to the maximal feasibility region, under CPDBL, the long-term time-averaged total storage cost is tunable and guaranteed to be under the given budget.

B. Regret Bound

Our second theorem provides an upper bound for the regret incurred by CPDBL over time.

Theorem 2: Under CPDBL, the regret $Reg(T)$ defined in (7) is upper bounded as follows:

$$Reg(T) \leq \frac{B}{V} + \frac{4 \sum_{n \in \mathcal{N}} K_n M_n}{T}$$

$$+ 2 \left(\sum_{n \in \mathcal{N}} K_n \sqrt{M_n \sum_{f \in \mathcal{F}} L_f} \right) \sqrt{\frac{6 \log T}{T + H_{\min}}}, \quad (18)$$

where $B \triangleq \sum_{n \in \mathcal{N}} (b_n^2 + \alpha^2 M_n^2)/2$ and $H_{\min} \triangleq \min_{n, f} H_{n, f}$.

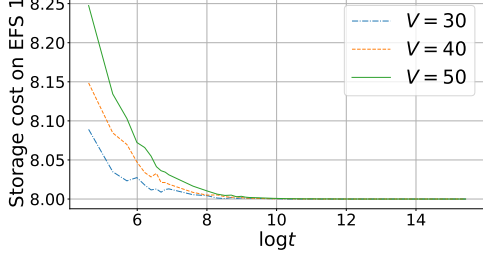
Remark 2: In (18), the term B/V is mainly incurred by balancing the cache hit reward and the storage cost constraints. Intuitively, the larger the value of V , CPDBL puts more focus on maximizing cache hit reward and hence a smaller regret. Nonetheless, this also comes with an increase in the total size of virtual queue backlogs, which is unfavorable for keeping storage costs under budget. In contrast, the smaller the value of V , the more sensitive CPDBL would be to the increase in storage costs. As a result, each EFS would constantly update its cached file set with files of different storage costs, leading to inferior cache hit rewards. In practice, the selection of the value of V depends on the design tradeoff of real systems. Besides, the other two terms in (18) are in the order of $O(\sqrt{(\log T)/(T + H_{\min})})$. Such two terms are mainly incurred by the online learning procedure with offline history information and collected online feedback. It turns out that, on the one hand, as the number of time slots T increases to infinity, the regret bound decreases to B/V . On the other hand, given a fixed number of time slots T , as the number of offline historical observations ($H_{n, f}$ with respect to each EFS n and file f) approaches infinity, the regret bound also reduces to B/V . In addition, with a sufficiently large number of historical observations and a large value of V , the incurred regret would approach zero as time goes by.

Proof Sketch: First, we introduce the notion of Lyapunov drift to characterize the change of virtual queue backlog sizes (in terms of the Lyapunov function) between consecutive time slots. Next, by taking the per-time-slot regret of CPDBL into the Lyapunov drift, we upper bound such a drift-plus-regret term by a linear function of the difference between the performances incurred by CPDBL and the optimal scheme. With the aid of an auxiliary scheme, we further transform the previous upper bound into a linear function of the difference between the performances of CPDBL and the auxiliary scheme. Finally, for the terms in the resulting bound, we leverage Chernoff-Hoeffding techniques and Jensen's inequality to bound each of them to complete the proof. More details of the proof are given in Appendix C.

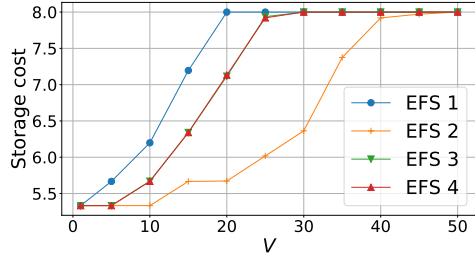
VI. NUMERICAL RESULTS

A. Simulation Settings

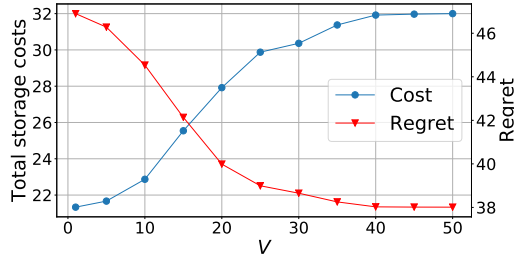
We consider a Fog-assisted IoT system with 1 CFS, 4 EFSs ($N = 4$) and 20 IoT users ($K = 20$). Each user is uniformly randomly assigned to one of the EFSs. The file set \mathcal{F} on the CFS consists of 20 files ($F = 20$) with different file sizes $L_f \in \{1, 2, 4, 8\}$. The storage capacity of each EFS is $M_n = 16$ units. We set the unit storage cost as $\alpha = 1$. We assume that each user k 's requests are generated from a Zipf distribution with a skewness parameter $\gamma \in [0.56, 1.2]$. Note that such skewness parameters are *unknown a priori* to the EFSs. We set the long-term budget b_n to be uniformly 8 units for each EFS $n \in \mathcal{N}$.



(a) Time-averaged storage cost on EFS 1.



(b) Storage costs on each EFS.



(c) Regret & total storage costs.

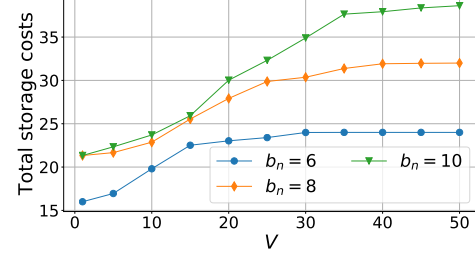
Fig. 4. Performance of CPDBL with different values of V .

B. Performance of CPDBL with A Fixed Time Horizon Length and Fixed Amounts of Offline History Information

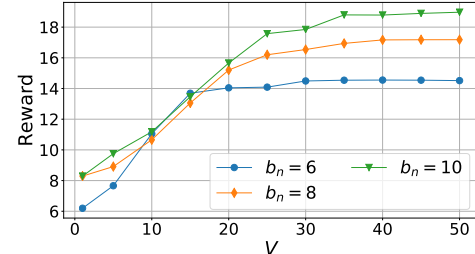
In this Subsection, we investigate the performance of CPDBL by fixing the time horizon length T as 5×10^6 time slots and the number of offline historical observations as $H_{n,f} = 1000$ for all $n \in \mathcal{N}, f \in \mathcal{F}$.

Performance of CPDBL under Different Values of V :

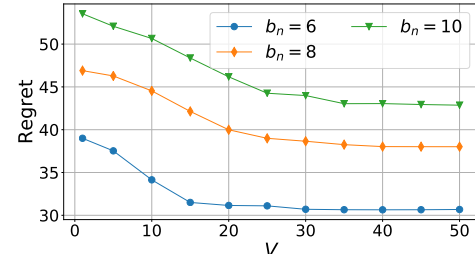
In Figure 4(a), we take the first EFS (EFS 1) as an example to investigate how the time-averaged storage cost on each EFS changes over time under different values of V . We see that on EFS 1, the time-averaged storage cost converges to the cost budget $b_1 = 8$ units as time goes by. Moreover, the greater the value of V , the longer the convergence time. For example, the convergence time extends from 4000 time slots to about 10000 time slots as the value of V increases from 30 to 50. This shows that: the larger the value of V , the longer the time for convergence. Figure 4(b) evaluates the time-averaged storage cost on each EFS incurred by CPDBL under different values of V . We see that as the value of parameter V increases, the storage cost on each EFS keeps increasing until it reaches the budget $b_n = 8$ units. Such results show that the long-term time-averaged storage cost constraints in (5) are always satisfied under CPDBL.



(a) Time-averaged total storage costs.



(b) Time-averaged total cache hit reward.



(c) Regret.

Fig. 5. Performance of CPDBL with different storage budgets (b_n).

Next, we switch to the regrets and total storage costs incurred by CPDBL with different values of V . As shown in Figure 4(c), we see a notable reduction in the regret as the value of V increases. Such results imply that CPDBL can achieve a lower regret with a larger value of V . Moreover, when the value of V is sufficiently large ($V \geq 40$), the regret value stabilizes at around 38.01. This verifies our previous analysis about the term B/V in the regret bound (18). Besides, as the value of V increases, we also see an increase in the total storage costs which eventually reaches the budget when $V \geq 40$. The results in Figures 4(b) and 4(c) verify the tunable tradeoff between the regret value and total storage costs.

Performance of CPDBL under Different Settings of Storage Cost Budget b_n : Next, we select different values for the storage cost budget b_n of each EFS n to investigate their impact on system performance. Figure 5 shows our simulation results. From Figure 5(a), we see that given $V = 50$, the time-averaged total storage costs increase by 60.93% as the value of b_n increases from 6 to 10. Under the same settings, Figure 5(b) shows that the time-averaged total cache hit reward increases by 30.71%. The reason is that with more budget, each EFS would store more files to further maximize the cache hit rewards. Figure 5(c) illustrates the regret under

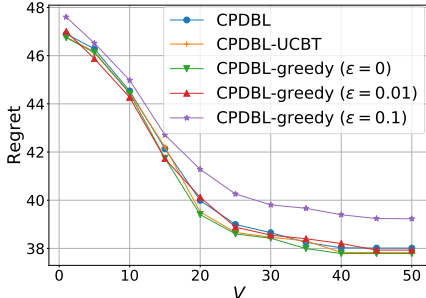


Fig. 6. Regret of CPDBL and its variants.

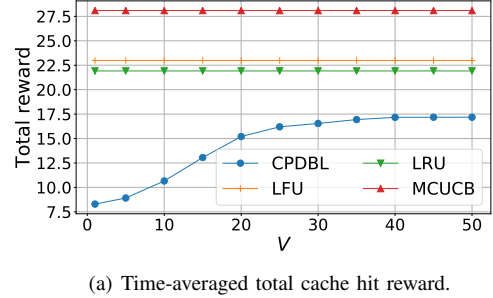
different storage cost budgets. The results verify our theoretical analysis (17) that the regret grows in proportion to the storage cost budget on each EFS. The reason is that under CPDBL, each EFS would explore more files when given more budget, thereby resulting in a higher regret.

CPDBL vs. Its Variants: In Section IV-B, the confidence radius in (10) measures the uncertainty in the empirical reward estimate. The greater the confidence radius, the greater the necessity of exploration for the corresponding file. Accordingly, each EFS is more prone to caching such under-explored files. To investigate how the regret changes with different degrees of exploration, we propose two types of variants for CPDBL: one leveraging ϵ -greedy method and the other employing UCB-like methods. More detail is specified as follows.

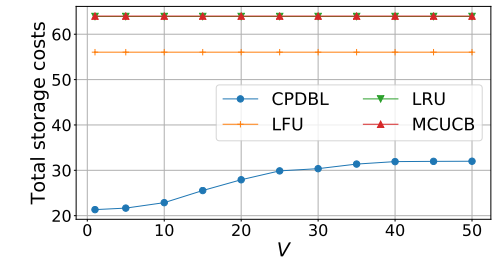
- ◊ **CPDBL-greedy:** CPDBL-greedy differs from CPDBL in the cache placement phase (lines 7-9 in Algorithm 1). Specifically, it replaces the HUCB1 estimates $\{\tilde{d}_{n,f}(t)\}_{n,f}$ with empirical means $\{\bar{d}_{n,f}(t)\}_{n,f}$ in function SETCACHEPLACEMENT. Recall that $\bar{d}_{n,f}(t)$ is the empirical mean that involves both offline historical observations and online feedbacks. Then it adopts ϵ -greedy method within the cache placement phase. With probability ϵ , each EFS n selects files uniformly randomly from subset $\mathcal{F}_{n,1}(t)$ to cache. With probability $1 - \epsilon$, files with the empirically highest reward estimates are chosen to be cached. Intuitively, CPDBL-greedy spends about a proportion ϵ of time for uniform exploration and the rest $(1 - \epsilon)$ proportion of time for exploitation.
- ◊ **CPDBL-UCBT:** CPDBL-UCBT replaces the HUCB1 estimate (line 4 in Algorithm 1) with *UCB1-tuned (UCBT)* estimate[32] while the rest remains the same as CPDBL.

We compare the regret value of CPDBL against CPDBL-greedy ($\epsilon \in \{0, 0.01, 0.1\}$) and CPDBL-UCBT in Figure 6 under different values of V . Regarding the variants of CPDBL, interestingly, although CPDBL-greedy with $\epsilon = 0$ discards the chance of uniform exploration in the online learning phase, it still achieves a regret performance that is close to CPDBL, CPDBL-UCBT, and CPDBL-greedy with $\epsilon = 0.01$. The reason is that CPDBL-greedy with $\epsilon = 0$ can resort to storage cost constraint guarantee in the online control phase to conduct enforced exploration. In comparison, the regret of CPDBL-greedy with $\epsilon = 0.1$ still performs inferior to other schemes due to its over-exploration.

CPDBL vs. Other Baseline Schemes: We also compare



(a) Time-averaged total cache hit reward.



(b) Time-averaged total storage costs.

Fig. 7. Comparison of CPDBL and baseline schemes.

the performance of CPDBL with three baseline schemes: LFU (*Least Frequently Used*)[33], LRU (*Least Recently Used*)[33], and MCUCB[28]. Below we show how each of them proceeds in detail, respectively.

- ◊ **LFU:** Under LFU, each EFS maintains a counter for each of its cached files. Each counter records the number of times that its corresponding file has been requested on the EFS. If a requested file is not in the cache, the requested file would be downloaded from the CFS and cached on the EFS by replacing the least frequently used files therein.
- ◊ **LRU:** Under LRU, each EFS records the most recently requested time slot for each of its cached files. If a requested file is not in the cache, the requested file would be downloaded from the CFS and cached on the EFS by replacing the least recently used files.
- ◊ **MCUCB:** Under MCUCB[10], a modified combinatorial UCB scheme is used to estimate file popularities and decide cache placement during each time slot.

We show the simulation results in Figure 7. The cache hit reward and total storage costs of the three baseline schemes (LFU, LRU, and MCUCB) remain constant given different values of V . This is because their decision making does not involve parameter V . From Figure 7, we see that CPDBL achieves the lowest cache hit reward while MCUCB achieves the highest cache hit reward. For example, given $V = 50$, compared to MCUCB, CPDBL achieves 38.85% less total cache hit reward and a 50.00% reduction in the total storage costs. Figure 7(b) shows that except CPDBL, the other three schemes fail to ensure the storage cost constraints (5).¹

¹Recall that the storage cost budget on each EFS is $b_n = 8$ units in our simulations. Accordingly, the total time-averaged storage costs of the four EFSs should not exceed 32 units. However, the total time-averaged storage costs are more than 55 units under the three baseline schemes.

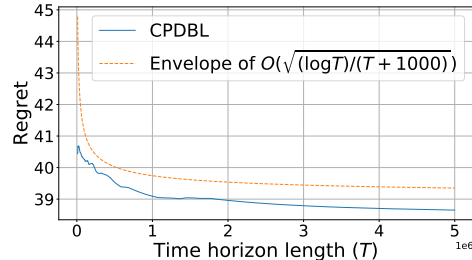
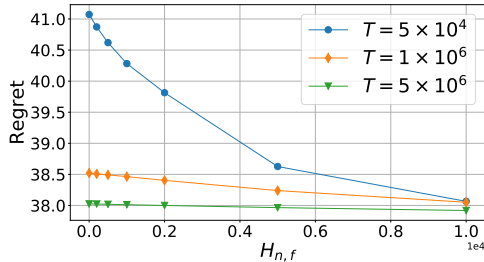
(a) Regret when $V = 30$ and $H_{n,f} = 1000$.(b) Regret with different values of T when $V = 50$.

Fig. 8. Regret of CPDBL.

C. Performance of CPDBL with Different Values of Time Horizon Length and Amounts of Offline History Information

In this Subsection, we investigate the impact of time horizon length T and numbers ($H_{n,f}$) of offline history observations² on the regret of CPDBL. The results are shown in Figure 8.

Figure 8(a) illustrates the regret of CPDBL under different values of time horizon length T when the number of offline historical observations is fixed as $H_{n,f} = 1000$. Specifically, as the value of T increases, the regret $Reg(T)$ decreases in the order of $O(\sqrt{\frac{\log T}{T+1000}})$.³ Next, we vary the values of $H_{n,f}$ from 0 to 10^4 and obtain the simulation results in Figure 8(b). We see that with more offline history information, CPDBL achieves a smaller regret. However, the longer the time horizon length (in term of T time slots), the lower the gain in regret reduction. For example, when each number $H_{n,f}$ of offline historical observations increases from 0 to 10^4 , the regret reduces by 7.32% under $T = 5 \times 10^4$ and by only 2.79% under $T = 5 \times 10^6$. All such results verify our theoretical analysis of Theorem 2 in Section V.

VII. CONCLUSION

In this paper, we considered the cache placement problem with unknown file popularities in caching-enabled Fog-assisted IoT systems. By formulating the problem as a constrained CMAB problem, we devised a novel proactive cache placement scheme called CPDBL with an effective integration of online control, online learning and offline history information.

²In our simulation, the value of $H_{n,f}$ is set to be identical for all $n \in \mathcal{N}$ and $f \in \mathcal{F}$.

³In Figure 8(a), we also provide a curve of $39 + 200\sqrt{\frac{\log T}{T+1000}}$ as an envelope of $O(\sqrt{\frac{\log T}{T+1000}})$ for illustration.

Results from our theoretical analysis and numerical simulations showed that our devised scheme achieves a near-optimal total cache hit reward under long-term storage cost constraints with a sublinear time-averaged regret. To the best of our knowledge, our work provides the first systematic study on the synergy of online control, online learning, and offline history information. Our results also revealed novel insights to the designers of cache-enabled Fog-assisted IoT systems.

REFERENCES

- [1] E. Bastug, M. Bennis, and M. Debbah, “Living on the edge: The role of proactive caching in 5g wireless networks,” *IEEE Communications Magazine*, vol. 52, no. 8, pp. 82–89, 2014.
- [2] S. Zhao, Z. Shao, H. Qian, and Y. Yang, “Online user-ap association with predictive scheduling in wireless caching networks,” in *Proceedings of IEEE GLOBECOM*, 2017.
- [3] Y. Jiang, M. Ma, M. Bennis, F. Zheng, and X. You, “A novel caching policy with content popularity prediction and user preference learning in fog-ran,” in *Proceedings of IEEE GLOBECOM Workshops*, 2017.
- [4] S. Zhao, Y. Yang, Z. Shao, X. Yang, H. Qian, and C.-X. Wang, “Femos: Fog-enabled multitier operations scheduling in dynamic wireless networks,” *IEEE Internet of Things Journal*, vol. 5, no. 2, pp. 1169–1183, 2018.
- [5] X. Gao, X. Huang, S. Bian, Z. Shao, and Y. Yang, “Pora: Predictive offloading and resource allocation in dynamic fog computing systems,” *IEEE Internet of Things Journal*, vol. 7, no. 1, pp. 72–87, 2020.
- [6] H. Pang, L. Gao, and L. Sun, “Joint optimization of data sponsoring and edge caching for mobile video delivery,” in *Proceedings of IEEE GLOBECOM*, 2016.
- [7] J. Kwak, Y. Kim, L. B. Le, and S. Chong, “Hybrid content caching in 5g wireless networks: Cloud versus edge caching,” *IEEE Transactions on Wireless Communications*, vol. 17, no. 5, pp. 3030–3045, 2018.
- [8] Y. Wang, W. Wang, Y. Cui, K. G. Shin, and Z. Zhang, “Distributed packet forwarding and caching based on stochastic network utility maximization,” *IEEE/ACM Transactions on Networking*, vol. 26, no. 3, pp. 1264–1277, 2018.
- [9] J. Xu, L. Chen, and P. Zhou, “Joint service caching and task offloading for mobile edge computing in dense networks,” in *Proceedings of IEEE INFOCOM*, 2018.
- [10] P. Blasco and D. Gündüz, “Learning-based optimization of cache content in a small cell base station,” in *Proceedings of IEEE ICC*, 2014.
- [11] ———, “Multi-armed bandit optimization of cache content in wireless infostation networks,” in *Proceedings of IEEE ISIT*, 2014.
- [12] S. Müller, O. Atan, M. van der Schaar, and A. Klein, “Smart caching in wireless small cell networks via contextual multi-armed bandits,” in *Proceedings of IEEE ICC*, 2016.
- [13] X. Zhang, G. Zheng, S. Lambotharan, M. R. Nakhai, and K.-K. Wong, “A learning approach to edge caching

with dynamic content library in wireless networks," in *Proceedings of IEEE GLOBECOM*, 2019.

[14] J. Song, M. Sheng, T. Q. Quek, C. Xu, and X. Wang, "Learning-based content caching and sharing for wireless networks," *IEEE Transactions on Communications*, vol. 65, no. 10, pp. 4309–4324, 2017.

[15] X. Xu, M. Tao, and C. Shen, "Collaborative multi-agent multi-armed bandit learning for small-cell caching," *arXiv preprint arXiv:2001.03835*, 2020.

[16] B. Bharath, K. G. Nagananda, and H. V. Poor, "A learning-based approach to caching in heterogenous small cell networks," *IEEE Transactions on Communications*, vol. 64, no. 4, pp. 1674–1686, 2016.

[17] F. Li, J. Liu, and B. Ji, "Combinatorial sleeping bandits with fairness constraints," in *Proceedings of IEEE INFOCOM*, 2019.

[18] P. Shivaswamy and T. Joachims, "Multi-armed bandit problems with history," in *Proceedings of AISTATS*, 2012.

[19] M. J. Neely, "Stochastic network optimization with application to communication and queueing systems," *Synthesis Lectures on Communication Networks*, vol. 3, no. 1, pp. 1–211, 2010.

[20] L. Li, G. Zhao, and R. S. Blum, "A survey of caching techniques in cellular networks: Research issues and challenges in content placement and delivery strategies," *IEEE Communications Surveys & Tutorials*, vol. 20, no. 3, pp. 1710–1732, 2018.

[21] H. Pang, J. Liu, X. Fan, and L. Sun, "Toward smart and cooperative edge caching for 5g networks: A deep learning based approach," in *Proceedings of IEEE/ACM IWQoS*, 2018.

[22] E. Baştug, M. Bennis, and M. Debbah, "A transfer learning approach for cache-enabled wireless networks," in *Proceedings of IEEE WiOpt*, 2015.

[23] A. Sengupta, S. Amuru, R. Tandon, R. M. Buehrer, and T. C. Clancy, "Learning distributed caching strategies in small cell networks," in *Proceedings of ISWCS*, 2014.

[24] A. Sadeghi, F. Sheikholeslami, A. G. Marques, and G. B. Giannakis, "Reinforcement learning for adaptive caching with dynamic storage pricing," *IEEE Journal on Selected Areas in Communications*, vol. 37, no. 10, pp. 2267–2281, 2019.

[25] Z. Zhu, T. Liu, S. Jin, and X. Luo, "Learn and pick right nodes to offload," in *Proceedings of IEEE GLOBECOM*, 2018.

[26] J. Yao and N. Ansari, "Energy-aware task allocation for mobile iot by online reinforcement learning," in *Proceedings of IEEE ICC*, 2019.

[27] A. Mukherjee, S. Misra, V. S. P. Chandra, and M. S. Obaidat, "Resource-optimized multiarmed bandit-based offload path selection in edge uav swarms," *IEEE Internet of Things Journal*, vol. 6, no. 3, pp. 4889–4896, 2018.

[28] W. Chen, Y. Wang, and Y. Yuan, "Combinatorial multi-armed bandit: General framework and applications," in *Proceedings of ICML*, 2013.

[29] A. Slivkins *et al.*, "Introduction to multi-armed bandits," *Foundations and Trends® in Machine Learning*, vol. 12, no. 1-2, pp. 1–286, 2019.

[30] S. Martello, D. Pisinger, and P. Toth, "Dynamic programming and strong bounds for the 0-1 knapsack problem," *Management Science*, vol. 45, no. 3, pp. 414–424, 1999.

[31] ———, "New trends in exact algorithms for the 0-1 knapsack problem," *European Journal of Operational Research*, vol. 123, no. 2, pp. 325–332, 2000.

[32] P. Auer, N. Cesa-Bianchi, and P. Fischer, "Finite-time analysis of the multiarmed bandit problem," *Machine Learning*, vol. 47, no. 2-3, pp. 235–256, 2002.

[33] D. Lee, J. Choi, J.-H. Kim, S. H. Noh, S. L. Min, Y. Cho, and C. S. Kim, "Lrfu: A spectrum of policies that subsumes the least recently used and least frequently used policies," *IEEE Transactions on Computers*, vol. 50, no. 12, pp. 1352–1361, 2001.

APPENDIX A ALGORITHM DEVELOPMENT

We define a Lyapunov function as follows:

$$L(\mathbf{Q}(t)) = \frac{1}{2} \sum_{n \in \mathcal{N}} (Q_n(t))^2, \quad (19)$$

in which $\mathbf{Q}(t) = (Q_1(t), Q_2(t), \dots, Q_N(t))$ is the vector of all virtual queues. Then we have

$$\begin{aligned} & L(\mathbf{Q}(t+1)) - L(\mathbf{Q}(t)) \\ &= \frac{1}{2} \sum_{n \in \mathcal{N}} [(Q_n(t+1))^2 - (Q_n(t))^2] \\ &\leq \frac{1}{2} \sum_{n \in \mathcal{N}} [b_n^2 + (C_n(t))^2 + 2Q_n(t)(C_n(t) - b_n)]. \end{aligned} \quad (20)$$

Since $C_n(t) = \sum_{f \in \mathcal{F}} \alpha L_f X_{n,f}(t) \leq \alpha M_n$, it follows that

$$\begin{aligned} & L(\mathbf{Q}(t+1)) - L(\mathbf{Q}(t)) \\ &\leq B + \sum_{n \in \mathcal{N}} Q_n(t)(C_n(t) - b_n), \end{aligned} \quad (21)$$

where $B \triangleq \frac{1}{2} \sum_{n \in \mathcal{N}} (b_n^2 + \alpha^2 M_n^2)$.

We consider an optimal cache placement scheme which makes *i.i.d.* placement decision $\mathbf{X}^*(t)$ in each time slot t , then the optimal time-averaged expected total reward of all EFSs is

$$R^* = \frac{1}{T} \sum_{t=0}^{T-1} \sum_{n \in \mathcal{N}} \mathbb{E} [\hat{R}_n(\mathbf{X}_n^*(t))]. \quad (22)$$

According to (7), the regret of cache placement scheme $\{\mathbf{X}(t)\}_t$ in the first T time slots is

$$Reg(T) = \frac{1}{T} \sum_{t=0}^{T-1} \sum_{n \in \mathcal{N}} \mathbb{E} [\hat{R}_n(\mathbf{X}_n^*(t)) - \hat{R}_n(\mathbf{X}_n(t))]. \quad (23)$$

By the definition of reward $\hat{R}_n(\cdot)$ in (4), it follows that

$$\begin{aligned} Reg(T) &= \frac{1}{T} \sum_{t=0}^{T-1} \sum_{n \in \mathcal{N}} \sum_{f \in \mathcal{F}} L_f (\mathbb{E} [D_{n,f}(t) X_{n,f}^*(t)] \\ &\quad - \mathbb{E} [D_{n,f}(t) X_{n,f}(t)]). \end{aligned} \quad (24)$$

Since the placement decision $X_{n,f}(t)$ is made when $D_{n,f}(t)$ is unknown, $X_{n,f}(t)$ is independent of the $D_{n,f}(t)$. On the other hand, $X_{n,f}^*(t)$ is *i.i.d.* over time slots and it is also independent of $D_{n,f}(t)$. Then by $\mathbb{E}[D_{n,f}(t)] = d_{n,f}$, we have

$$Reg(T) = \frac{1}{T} \sum_{t=0}^{T-1} \sum_{n \in \mathcal{N}} \sum_{f \in \mathcal{F}} L_f d_{n,f} \mathbb{E}[X_{n,f}^*(t) - X_{n,f}(t)]. \quad (25)$$

We define the one-slot regret as

$$\Delta_{Reg}(t) = \sum_{n \in \mathcal{N}} \sum_{f \in \mathcal{F}} L_f d_{n,f} (X_{n,f}^*(t) - X_{n,f}(t)). \quad (26)$$

The regret $Reg(T)$ can be expressed as

$$Reg(T) = \frac{1}{T} \sum_{t=0}^{T-1} \mathbb{E}[\Delta_{Reg}(t)]. \quad (27)$$

Then we define the Lyapunov drift-plus-regret as

$$\Delta_V(\mathbf{Q}(t)) = \mathbb{E}[L(\mathbf{Q}(t+1)) - L(\mathbf{Q}(t)) | \mathbf{Q}(t)] + V\mathbb{E}[\Delta_{Reg}(t) | \mathbf{Q}(t)]. \quad (28)$$

It follows by (21) and (26) that

$$\begin{aligned} \Delta_V(\mathbf{Q}(t)) &\leq B + V\mathbb{E}\left[\sum_{n \in \mathcal{N}} \sum_{f \in \mathcal{F}} L_f d_{n,f} X_{n,f}^*(t) | \mathbf{Q}(t)\right] \\ &\quad + \mathbb{E}\left[\sum_{n \in \mathcal{N}} Q_n(t) (C_n(t) - b_n) | \mathbf{Q}(t)\right] \\ &\quad - V\mathbb{E}\left[\sum_{n \in \mathcal{N}} \sum_{f \in \mathcal{F}} L_f d_{n,f} X_{n,f}(t) | \mathbf{Q}(t)\right]. \end{aligned} \quad (29)$$

Since $\tilde{d}_{n,f}(t)$ is the HUCB1 estimate of $d_{n,f}$ in time slot t and it satisfies $\tilde{d}_{n,f}(t) \in [0, K_n]$, we have

$$\begin{aligned} &\sum_{n \in \mathcal{N}} \sum_{f \in \mathcal{F}} L_f d_{n,f} X_{n,f}(t) \\ &= \sum_{n \in \mathcal{N}} \sum_{f \in \mathcal{F}} L_f \tilde{d}_{n,f}(t) X_{n,f}(t) \\ &\quad + \sum_{n \in \mathcal{N}} \sum_{f \in \mathcal{F}} L_f (d_{n,f} - \tilde{d}_{n,f}(t)) X_{n,f}(t) \\ &\stackrel{(a)}{\geq} \sum_{n \in \mathcal{N}} \sum_{f \in \mathcal{F}} L_f \tilde{d}_{n,f}(t) X_{n,f}(t) \\ &\quad - \sum_{n \in \mathcal{N}} K_n \sum_{f \in \mathcal{F}} L_f X_{n,f}(t) \\ &\stackrel{(b)}{\geq} \sum_{n \in \mathcal{N}} \sum_{f \in \mathcal{F}} L_f \tilde{d}_{n,f}(t) X_{n,f}(t) - \sum_{n \in \mathcal{N}} K_n M_n, \end{aligned} \quad (30)$$

where inequality (a) is because that $d_{n,f}, \tilde{d}_{n,f}(t) \in [0, K_n]$ and inequality (b) is because that $\sum_{f \in \mathcal{F}} L_f X_{n,f}(t) \leq M_n$.

Then it follows that

$$\begin{aligned} \Delta_V(\mathbf{Q}(t)) &\leq B + \sum_{n \in \mathcal{N}} V K_n M_n \\ &\quad + V\mathbb{E}\left[\sum_{n \in \mathcal{N}} \sum_{f \in \mathcal{F}} L_f d_{n,f} X_{n,f}^*(t) | \mathbf{Q}(t)\right] \\ &\quad + \mathbb{E}\left[\sum_{n \in \mathcal{N}} Q_n(t) (C_n(t) - b_n) | \mathbf{Q}(t)\right] \\ &\quad - V\mathbb{E}\left[\sum_{n \in \mathcal{N}} \sum_{f \in \mathcal{F}} L_f \tilde{d}_{n,f}(t) X_{n,f}(t) | \mathbf{Q}(t)\right]. \end{aligned} \quad (31)$$

Substituting (4) and (2) in, we have

$$\begin{aligned} \Delta_V(\mathbf{Q}(t)) &\leq B + \sum_{n \in \mathcal{N}} V K_n M_n - \sum_{n \in \mathcal{N}} Q_n(t) b_n \\ &\quad + V\mathbb{E}\left[\sum_{n \in \mathcal{N}} \sum_{f \in \mathcal{F}} L_f d_{n,f} X_{n,f}^*(t) | \mathbf{Q}(t)\right] \\ &\quad - \mathbb{E}\left[\sum_{n \in \mathcal{N}} \sum_{f \in \mathcal{F}} \tilde{w}_{n,f}(t) X_{n,f}(t) | \mathbf{Q}(t)\right]. \end{aligned} \quad (32)$$

where $\tilde{w}_{n,f}(t)$ is defined as

$$\tilde{w}_{n,f}(t) = L_f (V \tilde{d}_{n,f}(t) - \alpha Q_n(t)). \quad (33)$$

To minimize the upper bound of drift-plus-regret $\Delta_V(\mathbf{Q}(t))$ in (32), we approximately solve the following problem in each time slot t :

$$\begin{aligned} &\text{maximize}_{\mathbf{X}(t)} \sum_{n \in \mathcal{N}} \sum_{f \in \mathcal{F}} \tilde{w}_{n,f}(t) X_{n,f}(t) \\ &\text{subject to} \quad \sum_{f \in \mathcal{F}} L_f X_{n,f}(t) \leq M_n, \quad \forall n \in \mathcal{N}, \\ &\quad X_{n,f}(t) \in \{0, 1\}, \quad \forall n \in \mathcal{N}, f \in \mathcal{F}. \end{aligned} \quad (34)$$

Problem (34) can be decoupled into N subproblems. For each EFS $n \in \mathcal{N}$, we solve the following subproblem for the cache placement vector $\mathbf{X}_n(t)$ in time slot t :

$$\begin{aligned} &\text{maximize}_{\mathbf{X}_n(t)} \sum_{f \in \mathcal{F}} \tilde{w}_{n,f}(t) X_{n,f}(t) \\ &\text{subject to} \quad \sum_{f \in \mathcal{F}} L_f X_{n,f}(t) \leq M_n, \\ &\quad X_{n,f}(t) \in \{0, 1\}, \quad \forall f \in \mathcal{F}. \end{aligned} \quad (35)$$

APPENDIX B PROOF OF THEOREM 1

We consider a feasible cache placement scheme which makes *i.i.d.* placement decision $\mathbf{X}^\epsilon(t)$ in each time slot t such that

$$\mathbb{E}\left[\hat{C}_n(\mathbf{X}_n^\epsilon(t))\right] + \epsilon \leq b_n, \quad \forall n \in \mathcal{N} \quad (36)$$

holds for all time slots. Since our cache placement decision $\mathbf{X}(t)$ is the optimal solution to problem (34), based on (31) we have

$$\begin{aligned} \Delta_V(\mathbf{Q}(t)) &\leq B + \sum_{n \in \mathcal{N}} V K_n M_n \\ &+ V \mathbb{E} \left[\sum_{n \in \mathcal{N}} \sum_{f \in \mathcal{F}} L_f d_{n,f} X_{n,f}^*(t) | \mathbf{Q}(t) \right] \\ &+ \mathbb{E} \left[\sum_{n \in \mathcal{N}} Q_n(t) \left(\hat{C}_n(\mathbf{X}_n^\epsilon(t)) - b_n \right) | \mathbf{Q}(t) \right] \\ &- V \mathbb{E} \left[\sum_{n \in \mathcal{N}} \sum_{f \in \mathcal{F}} L_f \tilde{d}_{n,f}(t) X_{n,f}^\epsilon(t) | \mathbf{Q}(t) \right], \end{aligned} \quad (37)$$

where $B \triangleq \frac{1}{2} \sum_{n \in \mathcal{N}} (b_n^2 + \alpha^2 M_n^2)$. Since $\mathbf{X}^\epsilon(t)$ is independent of $\mathbf{Q}(t)$, we have

$$\begin{aligned} \Delta_V(\mathbf{Q}(t)) &\leq B + \sum_{n \in \mathcal{N}} V K_n M_n \\ &+ V \mathbb{E} \left[\sum_{n \in \mathcal{N}} \sum_{f \in \mathcal{F}} L_f d_{n,f} X_{n,f}^*(t) | \mathbf{Q}(t) \right] \\ &+ \sum_{n \in \mathcal{N}} Q_n(t) \mathbb{E} \left[\hat{C}_n(\mathbf{X}_n^\epsilon(t)) - b_n \right] \\ &- V \mathbb{E} \left[\sum_{n \in \mathcal{N}} \sum_{f \in \mathcal{F}} L_f \tilde{d}_{n,f}(t) X_{n,f}^\epsilon(t) | \mathbf{Q}(t) \right]. \end{aligned} \quad (38)$$

It follows by (36) that

$$\begin{aligned} \Delta_V(\mathbf{Q}(t)) &\leq B + \sum_{n \in \mathcal{N}} V K_n M_n - \epsilon \sum_{n \in \mathcal{N}} Q_n(t) \\ &+ V \mathbb{E} \left[\sum_{n \in \mathcal{N}} \sum_{f \in \mathcal{F}} L_f d_{n,f} X_{n,f}^*(t) | \mathbf{Q}(t) \right] \\ &- V \mathbb{E} \left[\sum_{n \in \mathcal{N}} \sum_{f \in \mathcal{F}} L_f \tilde{d}_{n,f}(t) X_{n,f}^\epsilon(t) | \mathbf{Q}(t) \right]. \end{aligned} \quad (39)$$

Since $\sum_{f \in \mathcal{F}} L_f d_{n,f} X_{n,f}^*(t) \leq K_n \sum_{f \in \mathcal{F}} L_f X_{n,f}^\epsilon(t) \leq K_n b_n$ and $\tilde{d}_{n,f} X_{n,f}^\epsilon(t) \geq 0$, we have

$$\Delta_V(\mathbf{Q}(t)) \leq B + V \sum_{n \in \mathcal{N}} 2 K_n M_n - \epsilon \sum_{n \in \mathcal{N}} Q_n(t). \quad (40)$$

Substituting (28) into above inequality, we have

$$\begin{aligned} \mathbb{E}[L(\mathbf{Q}(t+1)) - L(\mathbf{Q}(t)) | \mathbf{Q}(t)] + V \mathbb{E}[\Delta_{Reg}(t) | \mathbf{Q}(t)] \\ \leq B + V \sum_{n \in \mathcal{N}} 2 K_n M_n - \epsilon \sum_{n \in \mathcal{N}} Q_n(t). \end{aligned} \quad (41)$$

Taking expectation of both sides of above inequality and summing over time slots $\{0, 1, \dots, T' - 1\}$, we have

$$\begin{aligned} \mathbb{E}[L(\mathbf{Q}(T'))] - \mathbb{E}[L(\mathbf{Q}(0))] + V \sum_{t=0}^{T'-1} \mathbb{E}[\Delta_{Reg}(t)] \\ \leq T' B + T' V \sum_{n \in \mathcal{N}} 2 K_n M_n - \epsilon \sum_{t=0}^{T'-1} \sum_{n \in \mathcal{N}} \mathbb{E}[Q_n(t)]. \end{aligned} \quad (42)$$

Dividing both sides by $T' \epsilon$ and rearrange the items, we have

$$\begin{aligned} \frac{1}{T'} \sum_{t=0}^{T'-1} \sum_{n \in \mathcal{N}} \mathbb{E}[Q_n(t)] &\leq \frac{1}{\epsilon} \left(B + V \sum_{n \in \mathcal{N}} 2 K_n M_n \right) \\ &+ \frac{\mathbb{E}[L(\mathbf{Q}(0))]}{T' \epsilon} - \frac{\mathbb{E}[L(\mathbf{Q}(T'))]}{T' \epsilon} - \frac{V}{T' \epsilon} \sum_{t=0}^{T'-1} \mathbb{E}[\Delta_{Reg}(t)]. \end{aligned} \quad (43)$$

It follows by the fact $L(\mathbf{Q}(0)) = 0$, $L(\mathbf{Q}(T')) \geq 0$, and $\frac{1}{T'} \sum_{t=0}^{T'-1} \mathbb{E}[\Delta_{Reg}(t)] = Reg(T') \geq 0$ that

$$\frac{1}{T'} \sum_{t=0}^{T'-1} \sum_{n \in \mathcal{N}} \mathbb{E}[Q_n(t)] \leq \frac{B + V \sum_{n \in \mathcal{N}} 2 K_n M_n}{\epsilon}. \quad (44)$$

Let $T' \rightarrow \infty$ we obtain

$$\limsup_{T' \rightarrow \infty} \frac{1}{T'} \sum_{t=0}^{T'-1} \sum_{n \in \mathcal{N}} \mathbb{E}[Q_n(t)] \leq \frac{B + V \sum_{n \in \mathcal{N}} 2 K_n M_n}{\epsilon}. \quad (45)$$

This implies that $\limsup_{T' \rightarrow \infty} \frac{1}{T'} \sum_{t=0}^{T'-1} \mathbb{E}[Q_n(t)] < \infty$ and the virtual queueing process $\{Q_n\}_t$ defined in (13) is strongly stable for each EFS $n \in \mathcal{N}$. Thus the long-term time-averaged storage cost constraints (5) are satisfied. \blacksquare

APPENDIX C PROOF OF THEOREM 2

We consider the case when $\{\mathbf{X}^*(t)\}_t$ is an optimal scheme that makes *i.i.d.* cache placement decision $\mathbf{X}^*(t)$ in each time slot. Then $\mathbf{X}^*(t)$ satisfies

$$\mathbb{E}[\hat{C}_n(\mathbf{X}_n^*(t))] \leq b_n, \quad \forall n \in \mathcal{N} \quad (46)$$

for each time slot t . According to the inequality (21) and the definition (26), we have

$$\begin{aligned} L(\mathbf{Q}(t+1)) - L(\mathbf{Q}(t)) + V \Delta_{Reg}(t) \\ \leq B + \sum_{n \in \mathcal{N}} Q_n(t) (C_n(t) - b_n) \\ - V \sum_{n \in \mathcal{N}} \sum_{f \in \mathcal{F}} L_f d_{n,f} (X_{n,f}^*(t) - X_{n,f}(t)). \end{aligned} \quad (47)$$

The inequality above can be equivalently written as

$$\begin{aligned} L(\mathbf{Q}(t+1)) - L(\mathbf{Q}(t)) + V \Delta_{Reg}(t) \\ \leq B + \sum_{n \in \mathcal{N}} Q_n(t) \left(\hat{C}_n(\mathbf{X}_n^*(t)) - b_n \right) \\ + \sum_{n \in \mathcal{N}} \left(\sum_{f \in \mathcal{F}} V L_f d_{n,f} X_{n,f}^*(t) - Q_n(t) \hat{C}_n(\mathbf{X}_n^*(t)) \right) \\ - \sum_{n \in \mathcal{N}} \left(\sum_{f \in \mathcal{F}} V L_f d_{n,f} X_{n,f}(t) - Q_n(t) \hat{C}_n(\mathbf{X}_n(t)) \right). \end{aligned} \quad (48)$$

Substituting (2) in we have

$$\begin{aligned} L(\mathbf{Q}(t+1)) - L(\mathbf{Q}(t)) + V \Delta_{Reg}(t) \\ \leq B + \sum_{n \in \mathcal{N}} Q_n(t) \left(\hat{C}_n(\mathbf{X}_n^*(t)) - b_n \right) \\ + \sum_{n \in \mathcal{N}} \sum_{f \in \mathcal{F}} L_f (V d_{n,f} - \alpha Q_n(t)) X_{n,f}^*(t) \\ - \sum_{n \in \mathcal{N}} \sum_{f \in \mathcal{F}} L_f (V d_{n,f} - \alpha Q_n(t)) X_{n,f}(t). \end{aligned} \quad (49)$$

For each EFS $n \in \mathcal{N}$ and each file $f \in \mathcal{F}$, we define

$$w_{n,f}(t) = L_f(Vd_{n,f} - \alpha Q_n(t)). \quad (50)$$

Then inequality (49) can be expressed in a simplified form as:

$$\begin{aligned} & L(\mathbf{Q}(t+1)) - L(\mathbf{Q}(t)) + V\Delta_{Reg}(t) \\ & \leq B + \sum_{n \in \mathcal{N}} Q_n(t) (\hat{C}_n(\mathbf{X}_n^*(t)) - b_n) \\ & + \sum_{n \in \mathcal{N}} \sum_{f \in \mathcal{F}} w_{n,f}(t) (X_{n,f}^*(t) - X_{n,f}(t)). \end{aligned} \quad (51)$$

For simplicity of expression, we define

$$\Phi_1(t) = \sum_{n \in \mathcal{N}} \sum_{f \in \mathcal{F}} w_{n,f}(t) (X_{n,f}^*(t) - X_{n,f}(t)). \quad (52)$$

It follows that

$$\begin{aligned} & L(\mathbf{Q}(t+1)) - L(\mathbf{Q}(t)) + V\Delta_{Reg}(t) \\ & \leq B + \Phi_1(t) + \sum_{n \in \mathcal{N}} Q_n(t) (\hat{C}_n(\mathbf{X}_n^*(t)) - b_n). \end{aligned} \quad (53)$$

Taking conditional expectation of both sides, we have

$$\begin{aligned} & \mathbb{E}[L(\mathbf{Q}(t+1)) - L(\mathbf{Q}(t)) | \mathbf{Q}(t)] + V\mathbb{E}[\Delta_{Reg}(t) | \mathbf{Q}(t)] \\ & \leq B + \mathbb{E}[\Phi_1(t) | \mathbf{Q}(t)] \\ & + \mathbb{E}\left[\sum_{n \in \mathcal{N}} Q_n(t) (\hat{C}_n(\mathbf{X}_n^*(t)) - b_n) | \mathbf{Q}(t)\right] \\ & = B + \mathbb{E}[\Phi_1(t) | \mathbf{Q}(t)] \\ & + \sum_{n \in \mathcal{N}} Q_n(t) (\mathbb{E}[\hat{C}_n(\mathbf{X}_n^*(t))] - b_n). \end{aligned} \quad (55)$$

The last equality is because that $\hat{C}_n(\mathbf{X}_n^*(t))$ is independent of $\mathbf{Q}(t)$. It follows by inequalities (46) that

$$\begin{aligned} & \mathbb{E}[L(\mathbf{Q}(t+1)) - L(\mathbf{Q}(t)) | \mathbf{Q}(t)] \\ & + V\mathbb{E}[\Delta_{Reg}(t) | \mathbf{Q}(t)] \leq B + \mathbb{E}[\Phi_1(t) | \mathbf{Q}(t)]. \end{aligned} \quad (56)$$

Taking expectation of both sides, we have

$$\begin{aligned} & \mathbb{E}[L(\mathbf{Q}(t+1)) - L(\mathbf{Q}(t))] + V\mathbb{E}[\Delta_{Reg}(t)] \\ & \leq B + \mathbb{E}[\Phi_1(t)]. \end{aligned} \quad (57)$$

Summing the inequality above over time slots $\{0, 1, \dots, T-1\}$ and dividing both sides by TV , we have

$$\begin{aligned} & \frac{\mathbb{E}[L(\mathbf{Q}(T))] - \mathbb{E}[L(\mathbf{Q}(0))]}{TV} + \frac{1}{T} \sum_{t=0}^{T-1} \mathbb{E}[\Delta_{Reg}(t)] \\ & \leq \frac{B}{V} + \frac{1}{TV} \sum_{t=0}^{T-1} \mathbb{E}[\Phi_1(t)]. \end{aligned} \quad (58)$$

Since $L(\mathbf{Q}(0))$ and $L(\mathbf{Q}(T)) \geq 0$, it follows that

$$\begin{aligned} Reg(T) &= \frac{1}{T} \sum_{t=0}^{T-1} \mathbb{E}[\Delta_{Reg}(t)] \\ &\leq \frac{B}{V} + \frac{1}{TV} \sum_{t=0}^{T-1} \mathbb{E}[\Phi_1(t)]. \end{aligned} \quad (59)$$

A. Upper Bound of $\Phi_1(t)$

Next, we want to find the upper bound of $\mathbb{E}[\Phi_1(t)]$. Consider a cache placement scheme which makes placement decision $\mathbf{X}'(t) = (\mathbf{X}'_1(t), \mathbf{X}'_2(t), \dots, \mathbf{X}'_N(t))$ in each time slot t such that $\mathbf{X}'_n(t)$ is the optimal solution of the following problem:

$$\begin{aligned} & \text{maximize}_{\mathbf{X}'_n(t)} \sum_{f \in \mathcal{F}} w_{n,f}(t) X_{n,f}(t) \\ & \text{subject to} \quad \sum_{f \in \mathcal{F}} L_f X_{n,f}(t) \leq M_n, \\ & \quad X_{n,f}(t) \in \{0, 1\}, \forall f \in \mathcal{F}. \end{aligned} \quad (60)$$

Since $\mathbf{X}_n^*(t)$ is a feasible solution to problem (60), we have

$$\sum_{f \in \mathcal{F}} w_{n,f}(t) X'_{n,f}(t) \geq \sum_{f \in \mathcal{F}} w_{n,f}(t) X_{n,f}^*(t). \quad (61)$$

It follows that

$$\begin{aligned} \Phi_1(t) &= \sum_{n \in \mathcal{N}} \sum_{f \in \mathcal{F}} w_{n,f}(t) (X_{n,f}^*(t) - X_{n,f}(t)) \\ &\leq \sum_{n \in \mathcal{N}} \sum_{f \in \mathcal{F}} w_{n,f}(t) (X'_{n,f}(t) - X_{n,f}(t)) \\ &\leq \sum_{n \in \mathcal{N}} \sum_{f \in \mathcal{F}} w_{n,f}(t) (X'_{n,f}(t) - X_{n,f}(t)) \\ &+ \sum_{n \in \mathcal{N}} \sum_{f \in \mathcal{F}} \tilde{w}_{n,f}(t) (X_{n,f}(t) - X'_{n,f}(t)). \end{aligned} \quad (62)$$

The last inequality is due to that

$$\sum_{n \in \mathcal{N}} \sum_{f \in \mathcal{F}} \tilde{w}_{n,f}(t) X_{n,f}(t) \geq \sum_{n \in \mathcal{N}} \sum_{f \in \mathcal{F}} \tilde{w}_{n,f}(t) X'_{n,f}(t) \quad (63)$$

as $\mathbf{X}_n(t)$ is the optimal solution to problem (14) but $\mathbf{X}'_n(t)$ is only a feasible solution. Rearrange the right-hand side of (62), we obtain

$$\begin{aligned} \Phi_1(t) &\leq \sum_{n \in \mathcal{N}} \sum_{f \in \mathcal{F}} (\tilde{w}_{n,f}(t) - w_{n,f}) X_{n,f}(t) \\ &+ \sum_{n \in \mathcal{N}} \sum_{f \in \mathcal{F}} (w_{n,f} - \tilde{w}_{n,f}(t)) X'_{n,f}(t). \end{aligned} \quad (64)$$

By (33) and (50), we have

$$\begin{aligned} & \tilde{w}_{n,f}(t) - w_{n,f} \\ &= L_f (V\tilde{d}_{n,f}(t) - \alpha Q_n(t)) - L_f (Vd_{n,f} - \alpha Q_n(t)) \\ &= VL_f (\tilde{d}_{n,f}(t) - d_{n,f}). \end{aligned} \quad (65)$$

Substituting into (64), we obtain

$$\begin{aligned} \Phi_1(t) &\leq \sum_{n \in \mathcal{N}} \sum_{f \in \mathcal{F}} VL_f (\tilde{d}_{n,f}(t) - d_{n,f}) X_{n,f}(t) \\ &+ \sum_{n \in \mathcal{N}} \sum_{f \in \mathcal{F}} VL_f (d_{n,f} - \tilde{d}_{n,f}(t)) X'_{n,f}(t). \end{aligned} \quad (66)$$

Define

$$\Phi_2(t) = \sum_{n \in \mathcal{N}} \sum_{f \in \mathcal{F}} L_f (\tilde{d}_{n,f}(t) - d_{n,f}) X_{n,f}(t) \quad (67)$$

and

$$\Phi_3(t) = \sum_{n \in \mathcal{N}} \sum_{f \in \mathcal{F}} L_f (d_{n,f} - \tilde{d}_{n,f}(t)) X'_{n,f}(t), \quad (68)$$

The upper bound of $\Phi_1(t)$ in (66) can be written as

$$\Phi_1(t) \leq V(\Phi_2(t) + \Phi_3(t)). \quad (69)$$

B. Upper Bound of $\Phi_2(t)$

Define event $G_{n,f}(t) \triangleq \{\tilde{d}_{n,f}(t) \geq d_{n,f}\}$ for each $n \in \mathcal{N}$ and $f \in \mathcal{F}$, then we have

$$\begin{aligned} \Phi_2(t) &= \sum_{n \in \mathcal{N}} \sum_{f \in \mathcal{F}} L_f (\tilde{d}_{n,f}(t) - d_{n,f}) X_{n,f}(t) \\ &\quad \cdot (\mathbb{1}\{G_{n,f}(t)\} + \mathbb{1}\{G_{n,f}^c(t)\}) \\ &= \sum_{n \in \mathcal{N}} \sum_{f \in \mathcal{F}} L_f (\tilde{d}_{n,f}(t) - d_{n,f}) X_{n,f}(t) \mathbb{1}\{G_{n,f}(t)\} \\ &\quad + \sum_{n \in \mathcal{N}} \sum_{f \in \mathcal{F}} L_f (\tilde{d}_{n,f}(t) - d_{n,f}) X_{n,f}(t) \mathbb{1}\{G_{n,f}^c(t)\} \\ &\leq \sum_{n \in \mathcal{N}} \sum_{f \in \mathcal{F}} L_f (\tilde{d}_{n,f}(t) - d_{n,f}) X_{n,f}(t) \mathbb{1}\{G_{n,f}(t)\}. \end{aligned} \quad (70)$$

The last inequality is because that when event $G_{n,f}^c(t)$ happens, $\tilde{d}_{n,f}(t) < d_{n,f}$ and $(\tilde{d}_{n,f}(t) - d_{n,f}) \mathbb{1}\{G_{n,f}^c(t)\} < 0$. Next, we define

$$\phi_{2,n,f}(t) = (\tilde{d}_{n,f}(t) - d_{n,f}) X_{n,f}(t) \mathbb{1}\{G_{n,f}(t)\}. \quad (71)$$

Then we can express the upper bound of $\Phi_2(t)$ in (70) as

$$\Phi_2(t) \leq \sum_{n \in \mathcal{N}} \sum_{f \in \mathcal{F}} L_f \phi_{2,n,f}(t). \quad (72)$$

Let the first time when file f is cached at EFS n be time slot $t_{n,f}^{(1)}$. Define event $U_{n,f}(t) \triangleq \{\tilde{d}_{n,f}(t) - d_{n,f} > K_n \sqrt{\frac{3 \log t}{2(h_{n,f}(t) + H_{n,f})}}\}$ for each $n \in \mathcal{N}$ and $f \in \mathcal{F}$. Summing $\phi_{2,n,f}(t)$ over time slots $\{0, 1, \dots, T-1\}$ gives

$$\begin{aligned} &\sum_{t=0}^{T-1} \phi_{2,n,f}(t) \\ &= \sum_{t=0}^{T-1} (\tilde{d}_{n,f}(t) - d_{n,f}) X_{n,f}(t) \mathbb{1}\{G_{n,f}(t)\} \\ &\leq K_n X_{n,f}(t) \\ &\quad + \sum_{t=t_{n,f}^{(1)}+1}^{T-1} (\tilde{d}_{n,f}(t) - d_{n,f}) X_{n,f}(t) \mathbb{1}\{G_{n,f}(t)\} \\ &= K_n X_{n,f}(t) \\ &\quad + \sum_{t=t_{n,f}^{(1)}+1}^{T-1} (\tilde{d}_{n,f}(t) - d_{n,f}) X_{n,f}(t) \mathbb{1}\{G_{n,f}(t)\} \\ &\quad \cdot (\mathbb{1}\{U_{n,f}(t)\} + \mathbb{1}\{U_{n,f}^c(t)\}) \\ &= K_n X_{n,f}(t) \\ &\quad + \sum_{t=t_{n,f}^{(1)}+1}^{T-1} (\tilde{d}_{n,f}(t) - d_{n,f}) X_{n,f}(t) \\ &\quad \cdot \mathbb{1}\{G_{n,f}(t) \cap U_{n,f}(t)\} \\ &\quad + \sum_{t=t_{n,f}^{(1)}+1}^{T-1} (\tilde{d}_{n,f}(t) - d_{n,f}) X_{n,f}(t) \\ &\quad \cdot \mathbb{1}\{G_{n,f}(t) \cap U_{n,f}^c(t)\}. \end{aligned} \quad (73)$$

Define

$$\begin{aligned} \phi_{2,n,f}^{(1)}(t) &= (\tilde{d}_{n,f}(t) - d_{n,f}) X_{n,f}(t) \\ &\quad \cdot \mathbb{1}\{G_{n,f}(t) \cap U_{n,f}(t)\} \end{aligned} \quad (74)$$

and

$$\begin{aligned} \phi_{2,n,f}^{(2)}(t) &= (\tilde{d}_{n,f}(t) - d_{n,f}) X_{n,f}(t) \\ &\quad \cdot \mathbb{1}\{G_{n,f}(t) \cap U_{n,f}^c(t)\}, \end{aligned} \quad (75)$$

then inequality (73) can be written as

$$\begin{aligned} \sum_{t=0}^{T-1} \phi_{2,n,f}(t) &\leq K_n X_{n,f}(t) \\ &\quad + \sum_{t=t_{n,f}^{(1)}+1}^{T-1} \phi_{2,n,f}^{(1)}(t) + \sum_{t=t_{n,f}^{(1)}+1}^{T-1} \phi_{2,n,f}^{(2)}(t). \end{aligned} \quad (76)$$

First, we consider the upper bound of $\sum_{t=t_{n,f}^{(1)}+1}^{T-1} \phi_{2,n,f}^{(1)}(t)$. According to (74) we have

$$\begin{aligned} \sum_{t=t_{n,f}^{(1)}+1}^{T-1} \phi_{2,n,f}^{(1)}(t) &= \sum_{t=t_{n,f}^{(1)}+1}^{T-1} (\tilde{d}_{n,f}(t) - d_{n,f}) X_{n,f}(t) \\ &\quad \cdot \mathbb{1}\{G_{n,f}(t) \cap U_{n,f}(t)\}. \end{aligned} \quad (77)$$

When $U_{n,f}(t) = \{\tilde{d}_{n,f}(t) - d_{n,f} > K_n \sqrt{\frac{3 \log t}{2(h_{n,f}(t) + H_{n,f})}}\}$ occurs, we consider two cases:

- (i) If $\tilde{d}_{n,f}(t) = \min \left\{ \tilde{d}_{n,f}(t) + K_n \sqrt{\frac{3 \log t}{2(h_{n,f}(t) + H_{n,f})}}, K_n \right\} = K_n$, then $\tilde{d}_{n,f}(t) \geq d_{n,f}$, i.e., event $G_{n,f}(t)$ happens.
- (ii) If $\tilde{d}_{n,f}(t) = \min \left\{ \tilde{d}_{n,f}(t) + K_n \sqrt{\frac{3 \log t}{2(h_{n,f}(t) + H_{n,f})}}, K_n \right\} = \tilde{d}_{n,f}(t) + K_n \sqrt{\frac{3 \log t}{2(h_{n,f}(t) + H_{n,f})}}$, then $\tilde{d}_{n,f}(t) > d_{n,f} + 2K_n \sqrt{\frac{3 \log t}{2(h_{n,f}(t) + H_{n,f})}}$, i.e., event $G_{n,f}(t)$ still happens.

In summary, event $U_{n,f}(t)$ and $G_{n,f}(t)$ satisfy that $U_{n,f}(t) \subset G_{n,f}(t)$, or equivalently $\mathbb{1}\{G_{n,f}(t) \cap U_{n,f}(t)\} = \mathbb{1}\{U_{n,f}(t)\}$. Thus we have

$$\begin{aligned} &\sum_{t=t_{n,f}^{(1)}+1}^{T-1} \phi_{2,n,f}^{(1)}(t) \\ &= \sum_{t=t_{n,f}^{(1)}+1}^{T-1} (\tilde{d}_{n,f}(t) - d_{n,f}) X_{n,f}(t) \mathbb{1}\{U_{n,f}(t)\}. \end{aligned} \quad (78)$$

Since $\tilde{d}_{n,f}(t), d_{n,f} \in [0, K_n]$, we have $\tilde{d}_{n,f}(t) - d_{n,f} \leq K_n$. Then it follows that

$$\sum_{t=t_{n,f}^{(1)}+1}^{T-1} \phi_{2,n,f}^{(1)}(t) \leq \sum_{t=t_{n,f}^{(1)}+1}^{T-1} K_n X_{n,f}(t) \mathbb{1}\{U_{n,f}(t)\}. \quad (79)$$

Taking expectation of both sides, we have

$$\begin{aligned}
& \sum_{t=t_{n,f}+1}^{T-1} \mathbb{E} \left[\phi_{2,n,f}^{(1)}(t) \right] \\
& \leq \sum_{t=t_{n,f}^{(1)}+1}^{T-1} K_n X_{n,f}(t) \Pr \{ U_{n,f}(t) \} \\
& = \sum_{t=t_{n,f}^{(1)}+1}^{T-1} K_n X_{n,f}(t) \\
& \quad \cdot \Pr \left\{ \bar{d}_{n,f}(t) - d_{n,f} > K_n \sqrt{\frac{3 \log t}{2(h_{n,f}(t) + H_{n,f})}} \right\}. \tag{80}
\end{aligned}$$

Using the Chernoff-Hoeffding bound, we have

$$\begin{aligned}
& \Pr \left\{ \bar{d}_{n,f}(t) - d_{n,f} > K_n \sqrt{\frac{3 \log t}{2(h_{n,f}(t) + H_{n,f})}} \right\} \\
& \leq \exp \left(-\frac{2(h_{n,f}(t) + H_{n,f})^2}{(h_{n,f}(t) + H_{n,f})K_n^2} \cdot K_n^2 \frac{3 \log t}{2(h_{n,f}(t) + H_{n,f})} \right) \\
& = \exp(-3 \log t). \tag{81}
\end{aligned}$$

Then it follows that

$$\begin{aligned}
& \sum_{n \in \mathcal{N}} \sum_{f \in \mathcal{F}} \sum_{t=t_{n,f}^{(1)}+1}^{T-1} L_f \mathbb{E} \left[\phi_{2,n,f}^{(1)}(t) \right] \\
& \leq \sum_{t=1}^{\infty} \sum_{n \in \mathcal{N}} \sum_{f \in \mathcal{F}} L_f K_n X_{n,f}(t) t^{-3} \\
& \leq \sum_{t=1}^{\infty} \sum_{n \in \mathcal{N}} K_n M_n t^{-3} \\
& = \sum_{n \in \mathcal{N}} K_n M_n \left(1 + \sum_{t=2}^{\infty} t^{-3} \right) \\
& \leq \sum_{n \in \mathcal{N}} K_n M_n \left(1 + \int_1^{\infty} t^{-3} dt \right) = \frac{3}{2} \sum_{n \in \mathcal{N}} K_n M_n. \tag{82}
\end{aligned}$$

Next, we consider the upper bound of $\sum_{t=t_{n,f}^{(1)}+1}^{T-1} \phi_{2,n,f}^{(2)}(t)$. According to (75) we have

$$\begin{aligned}
\sum_{t=t_{n,f}^{(1)}+1}^{T-1} \phi_{2,n,f}^{(2)}(t) & = \sum_{t=t_{n,f}^{(1)}+1}^{T-1} \left(\tilde{d}_{n,f}(t) - d_{n,f} \right) X_{n,f}(t) \\
& \quad \cdot \mathbb{1} \{ G_{n,f}(t) \cap U_{n,f}^c(t) \}. \tag{83}
\end{aligned}$$

If event $U_{n,f}^c(t)$ happens, then we have

$$\begin{aligned}
\tilde{d}_{n,f}(t) & = \min \left\{ \bar{d}_{n,f}(t) + K_n \sqrt{\frac{3 \log t}{2(h_{n,f}(t) + H_{n,f})}}, K_n \right\} \\
& \leq \bar{d}_{n,f}(t) + K_n \sqrt{\frac{3 \log t}{2(h_{n,f}(t) + H_{n,f})}}, \tag{84}
\end{aligned}$$

and thus

$$\tilde{d}_{n,f}(t) - d_{n,f} = \left(\tilde{d}_{n,f}(t) - \bar{d}_{n,f}(t) \right)$$

$$+ (\bar{d}_{n,f}(t) - d_{n,f}) \leq 2K_n \sqrt{\frac{3 \log t}{2(h_{n,f}(t) + H_{n,f})}}. \tag{85}$$

Then by (85) and $X_{n,f}(t) \leq 1$ we have

$$\begin{aligned}
& \sum_{t=t_{n,f}^{(1)}+1}^{T-1} \phi_{2,n,f}^{(2)}(t) \\
& = \sum_{t=t_{n,f}^{(1)}+1}^{T-1} 2K_n X_{n,f}(t) \sqrt{\frac{3 \log t}{2(h_{n,f}(t) + H_{n,f})}} \\
& \quad \cdot \mathbb{1} \{ G_{n,f}(t) \cap U_{n,f}^c(t) \} \\
& \leq \sum_{t=t_{n,f}^{(1)}+1}^{T-1} 2K_n X_{n,f}(t) \sqrt{\frac{3 \log t}{2(h_{n,f}(t) + H_{n,f})}} \\
& \leq \sum_{t=t_{n,f}^{(1)}+1}^{T-1} K_n \sqrt{6 \log T} \frac{X_{n,f}(t)}{\sqrt{h_{n,f}(t) + H_{n,f}}}. \tag{86}
\end{aligned}$$

Since $h_{n,f}(t) \leq T$, we have

$$\begin{aligned}
\frac{1}{\sqrt{h_{n,f}(t) + H_{n,f}}} & = \sqrt{\frac{h_{n,f}(t)}{h_{n,f}(t) + H_{n,f}}} \cdot \frac{1}{\sqrt{h_{n,f}(t)}} \\
& \leq \sqrt{\frac{T}{T + H_{n,f}}} \cdot \frac{1}{\sqrt{h_{n,f}(t)}} \tag{87}
\end{aligned}$$

Then it follows that

$$\sum_{t=t_{n,f}^{(1)}+1}^{T-1} \phi_{2,n,f}^{(2)}(t) \leq \sum_{t=t_{n,f}^{(1)}+1}^{T-1} K_n \sqrt{\frac{6T \log T}{T + H_{n,f}}} \frac{1}{\sqrt{h_{n,f}(t)}}. \tag{88}$$

Let $t_{n,f}^{(i)}$ be the i th time slot when file f is cached at EFS n , then $t_{n,f}^{(h_{n,f}(T))}$ is the time slot when file f is lastly cached before time slot T . Then we have

$$\begin{aligned}
\sum_{t=t_{n,f}^{(1)}+1}^{T-1} \frac{1}{\sqrt{h_{n,f}(t)}} & = \sum_{i=2}^{h_{n,f}(T)} \frac{1}{\sqrt{h_{n,f}(t_{n,f}^{(i)})}} \\
& = \sum_{i=2}^{h_{n,f}(T)} \frac{1}{\sqrt{i-1}} = \sum_{i=1}^{h_{n,f}(T)-1} \frac{1}{\sqrt{i}} \\
& \leq \int_1^{h_{n,f}(T)} \frac{1}{\sqrt{i}} di = 2 \left(\sqrt{h_{n,f}(T)} - 1 \right) \\
& \leq 2\sqrt{h_{n,f}(T)}. \tag{89}
\end{aligned}$$

It follows that

$$\sum_{t=t_{n,f}^{(1)}+1}^{T-1} \phi_{2,n,f}^{(2)}(t) \leq 2K_n \sqrt{\frac{6T \log T}{T + H_{n,f}}} \sqrt{h_{n,f}(T)}. \tag{90}$$

Combining (72), (76), (82) and (90) we have

$$\begin{aligned}
\sum_{t=0}^{T-1} \mathbb{E}[\Phi_2(t)] &\leq \sum_{n \in \mathcal{N}} \sum_{f \in \mathcal{F}} L_f \sum_{t=0}^{T-1} \mathbb{E}[\phi_{2,n,f}(t)] \\
&\leq \frac{5}{2} \sum_{n \in \mathcal{N}} K_n M_n \\
&\quad + 2 \sum_{n \in \mathcal{N}} \sum_{f \in \mathcal{F}} L_f K_n \sqrt{\frac{6T \log T}{T + H_{n,f}}} \sqrt{h_{n,f}(T)} \\
&\leq \frac{5}{2} \sum_{n \in \mathcal{N}} K_n M_n \\
&\quad + 2 \sqrt{\frac{6T \log T}{T + H_{\min}}} \sum_{n \in \mathcal{N}} K_n \sum_{f \in \mathcal{F}} L_f \sqrt{h_{n,f}(T)},
\end{aligned} \tag{91}$$

where $H_{\min} \triangleq \min_{n,f} H_{n,f} \geq 0$. The last inequality is because that $\sum_{f \in \mathcal{F}} L_f X_{n,f}(t) \leq M_n$ for each $n \in \mathcal{N}$. On the other hand, by Jensen's inequality we have

$$\begin{aligned}
\sum_{f \in \mathcal{F}} \frac{L_f}{\sum_{f \in \mathcal{F}} L_f} \sqrt{h_{n,f}(T)} &\leq \sqrt{\frac{\sum_{f \in \mathcal{F}} L_f h_{n,f}(T)}{\sum_{f \in \mathcal{F}} L_f}} \\
&\leq \sqrt{\frac{M_n T}{\sum_{f \in \mathcal{F}} L_f}}.
\end{aligned} \tag{92}$$

Thus it follows that

$$\begin{aligned}
\sum_{t=0}^{T-1} \mathbb{E}[\Phi_2(t)] &\leq \frac{5}{2} \sum_{n \in \mathcal{N}} K_n M_n \\
&\quad + 2 \left(\sum_{n \in \mathcal{N}} K_n \sqrt{M_n \sum_{f \in \mathcal{F}} L_f} \right) \sqrt{\frac{6T^2 \log T}{T + H_{\min}}}.
\end{aligned} \tag{93}$$

C. Upper Bound of $\Phi_3(t)$

Recall by (68) and $G_{n,f}(t) \triangleq \{\tilde{d}_{n,f}(t) \geq d_{n,f}\}$ that

$$\begin{aligned}
\Phi_3(t) &= \sum_{n \in \mathcal{N}} \sum_{f \in \mathcal{F}} L_f (d_{n,f} - \tilde{d}_{n,f}(t)) X'_{n,f}(t) \\
&= \sum_{n \in \mathcal{N}} \sum_{f \in \mathcal{F}} L_f (d_{n,f} - \tilde{d}_{n,f}(t)) X'_{n,f}(t) \\
&\quad \cdot (\mathbb{1}\{G_{n,f}(t)\} + \mathbb{1}\{G_{n,f}^c(t)\}) \\
&\leq \sum_{n \in \mathcal{N}} \sum_{f \in \mathcal{F}} L_f (d_{n,f} - \tilde{d}_{n,f}(t)) X'_{n,f}(t) \mathbb{1}\{G_{n,f}^c(t)\}.
\end{aligned} \tag{94}$$

Define

$$\phi_{3,n,f}(t) = (d_{n,f} - \tilde{d}_{n,f}(t)) X'_{n,f}(t) \mathbb{1}\{G_{n,f}^c(t)\}, \tag{95}$$

then the upper bound of $\Phi_3(t)$ in (94) can be written as

$$\Phi_3(t) \leq \sum_{n \in \mathcal{N}} \sum_{f \in \mathcal{F}} L_f \phi_{3,n,f}(t). \tag{96}$$

We consider the case when $t \leq t_{n,f}^{(1)}$ and $t \geq t_{n,f}^{(1)} + 1$ separately. When $t \leq t_{n,f}^{(1)}$, $\tilde{d}_{n,f}(t) = K_n$ and the event $G_{n,f}^c(t) = \{\tilde{d}_{n,f}(t) < d_{n,f}\}$ will not happen since $d_{n,f} \leq K_n$. Thus $\phi_{3,n,f}(t) = 0$ when $t \leq t_n$.

When $t \geq t_{n,f}^{(1)} + 1$, suppose event $G_{n,f}^c(t)$ happens. Then we have $\tilde{d}_{n,f}(t) < d_{n,f} \leq K_n$, which implies that $\tilde{d}_{n,f}(t) = \tilde{d}_{n,f}(t) + K_n \sqrt{\frac{3 \log t}{2(h_{n,f}(t) + H_{n,f})}}$ and it follows that $d_{n,f} > \tilde{d}_{n,f}(t) + K_n \sqrt{\frac{3 \log t}{2(h_{n,f}(t) + H_{n,f})}}$. Thus we can bound $\mathbb{E}[\phi_{3,n,f}(t)]$ as follows:

$$\begin{aligned}
&\mathbb{E}[\phi_{3,n,f}(t)] \\
&= \mathbb{E}[(d_{n,f} - \tilde{d}_{n,f}(t)) X'_{n,f}(t) \mathbb{1}\{G_{n,f}^c(t)\}] \\
&\leq \mathbb{E}[K_n X'_{n,f}(t) \mathbb{1}\{G_{n,f}^c(t)\}] \\
&= K_n X'_{n,f}(t) \mathbb{E}[\mathbb{1}\{G_{n,f}^c(t)\}] \\
&= K_n X'_{n,f}(t) \Pr\{G_{n,f}^c(t)\} \\
&\leq K_n X'_{n,f}(t) \\
&\quad \cdot \Pr\left\{d_{n,f} > \tilde{d}_{n,f}(t) + K_n \sqrt{\frac{3 \log t}{2(h_{n,f}(t) + H_{n,f})}}\right\}.
\end{aligned} \tag{97}$$

By Chernoff-Hoeffding bound,

$$\begin{aligned}
&\Pr\left\{d_{n,f} > \tilde{d}_{n,f}(t) + K_n \sqrt{\frac{3 \log t}{2(h_{n,f}(t) + H_{n,f})}}\right\} \\
&= \Pr\left\{\tilde{d}_{n,f}(t) < d_{n,f} - K_n \sqrt{\frac{3 \log t}{2(h_{n,f}(t) + H_{n,f})}}\right\} \\
&\leq \exp\left(-\frac{2(h_{n,f}(t) + H_{n,f})^2}{(h_{n,f}(t) + H_{n,f})K_n^2} \cdot K_n^2 \frac{3 \log t}{2(h_{n,f}(t) + H_{n,f})}\right) \\
&= \exp(-3 \log t) = t^{-3}.
\end{aligned} \tag{98}$$

Thus we have

$$\mathbb{E}[\phi_{3,n,f}(t)] \leq K_n X'_{n,f}(t) t^{-3}. \tag{99}$$

Based on the inequality above we have

$$\begin{aligned}
&\sum_{t=0}^{T-1} \sum_{f \in \mathcal{F}} L_f \mathbb{E}[\phi_{3,n,f}(t)] \\
&\leq K_n \sum_{t=t_{n,f}^{(1)}+1}^{T-1} \sum_{f \in \mathcal{F}} L_f X'_{n,f}(t) t^{-3} \\
&\leq K_n \sum_{t=t_{n,f}^{(1)}+1}^{T-1} M_n t^{-3},
\end{aligned} \tag{100}$$

where the last inequality is because that $\sum_{f \in \mathcal{F}} L_f X'_{n,f}(t) \leq M_n$. Then it follows that

$$\begin{aligned}
&\sum_{t=0}^{T-1} \sum_{f \in \mathcal{F}} L_f \mathbb{E}[\phi_{3,n,f}(t)] \\
&\leq K_n M_n \sum_{t=t_{n,f}^{(1)}+1}^{T-1} t^{-3} \leq K_n M_n \sum_{t=1}^{\infty} t^{-3} \\
&\leq K_n M_n \left(1 + \sum_{t=2}^{\infty} t^{-3}\right) \\
&\leq K_n M_n \left(1 + \int_1^{\infty} t^{-3} dt\right) = \frac{3}{2} K_n M_n.
\end{aligned} \tag{101}$$

By (96) and (101) we have

$$\begin{aligned} \sum_{t=0}^{T-1} \mathbb{E} [\Phi_3(t)] &\leq \sum_{n \in \mathcal{N}} \sum_{t=0}^{T-1} \sum_{f \in \mathcal{F}} L_f \mathbb{E} [\phi_{3,n,f}(t)] \\ &\leq \sum_{n \in \mathcal{N}} \frac{3}{2} K_n M_n. \end{aligned} \quad (102)$$

Combining (69), (93) and (102), we obtain

$$\begin{aligned} &\sum_{t=0}^{T-1} \mathbb{E} [\Phi_1(t)] \\ &\leq V \left(\sum_{t=0}^{T-1} \mathbb{E} [\Phi_2(t)] + \sum_{t=0}^{T-1} \mathbb{E} [\Phi_3(t)] \right) \\ &\leq 4V \sum_{n \in \mathcal{N}} K_n M_n \\ &\quad + 2V \left(\sum_{n \in \mathcal{N}} K_n \sqrt{M_n \sum_{f \in \mathcal{F}} L_f} \right) \sqrt{\frac{6T^2 \log T}{T + H_{\min}}}. \end{aligned} \quad (103)$$

Substituting (103) into (59) we obtain the regret upper bound as follows:

$$\begin{aligned} \text{Reg}(T) &\leq \frac{B}{V} + \frac{4 \sum_{n \in \mathcal{N}} K_n M_n}{T} \\ &\quad + 2 \left(\sum_{n \in \mathcal{N}} K_n \sqrt{M_n \sum_{f \in \mathcal{F}} L_f} \right) \sqrt{\frac{6 \log T}{T + H_{\min}}}, \end{aligned} \quad (104)$$

where $B = \frac{1}{2} \sum_{n \in \mathcal{N}} (b_n^2 + \alpha^2 M_n^2)$. ■